Synthetic, Spectroscopic and Structural Studies on Phosphine-stabilised [$\mathrm{PPh_3}$, $\mathrm{Ph_2PCH_2PPh_2}$, $\mathrm{Ph_2P(CH_2)_4PPh_2}$, $\mathrm{(Ph_2P)C_5H_4N}$] Main Group Element–Iron–Silicon Chain Complexes*

Pierre Braunstein,[a] **Michael Knorr,**[a] **Martin Strampfer,**[a] **André DeCian**[b] **and Jean Fischer**[b]

[a] *Laboratoire de Chimie de Coordination, Associé au CNRS (URA 0416), Université Louis Pasteur, 4 rue Blaise Pascal, F-67070 Strasbourg Cédex, France*

[b] *Laboratoire de Cristallochimie et de Chimie Structurale, Associé au CNRS (URA 424), Université Louis Pasteur, 4 rue Blaise Pascal, F-67070 Strasbourg Cédex, France*

The reaction between $\mathrm{K[Fe(CO)_3(PPh_3)\{Si(OMe)_3\}]}$ and $\mathrm{InX_3}$ (X = Cl or Br) gave complexes of the type $\mathrm{Fe{-}In(\mu{-}X)_2In{-}Fe}$. The chloride-bridged complexes easily form adducts with two-electron donors such as pyridine or $\mathrm{O{=}PPh_3}$. The structure of the chlorobenzene solvate of *mer*-$\mathrm{[(Ph_3P)(OC)_3Fe\{\mu{-}Si(OMe)_2(OMe)\}InCl_2(O{=}PPh_3)]}$ was determined by X-ray diffraction. An oxygen–indium interaction was established which results in a four-membered Fe–Si–O–In ring. This interaction was also evidenced by a variable-temperature ^{1}H NMR study. The reaction of 2 equivalents of $\mathrm{K[Fe(CO)_3(PPh_3)\{Si(OMe)_3\}]}$ with $\mathrm{InCl_3}$ gave the trinuclear complex *mer*-$\mathrm{InCl\{Fe(CO)_3(PPh_3)[\mu{-}Si(OMe)_2(OMe)]\}_2]}$ which reacts with $\mathrm{O{=}PPh_3}$ to yield *mer*-$\mathrm{[InCl(O{=}PPh_3)\{Fe(CO)_3(PPh_3)[Si(OMe)_3]\}_2]}$. With $\mathrm{GaCl_3}$ and $\mathrm{K[(CO)_3\{Si(OMe)_3\}(dppm{-}}$*P*$\mathrm{)]}$ (dppm = $\mathrm{Ph_2PCH_2PPh_2}$) the complex *mer*-$\mathrm{[\{(MeO)_3Si\}(OC)_3Fe(\mu{-}dppm)GaCl_2]}$ was formed, in which the Fe–Ga bond is stabilised by a bridging dppm ligand. The corresponding complex *mer*-$\mathrm{[\{(MeO)_3Si\}(OC)_3Fe(\mu{-}dppm)InCl_2]}$ was used in the synthesis of trimetallic complexes of the type *mer*-$\mathrm{[\{(MeO)_3Si\}(OC)_3Fe(\mu{-}dppm)InCl(M')]}$ [$\mathrm{M' = Mo(C_5H_4Me)(CO)_3}$ or $\mathrm{W(C_5H_5)(CO)_3}$]. The structure of the chlorobenzene solvate of the molybdenum complex was determined by X-ray diffraction. Reaction of $\mathrm{K[Fe(CO)_3\{Si(OMe)_3\}(dppm{-}}$*P*$\mathrm{)]}$ and $\mathrm{[SnCl_2Ph_2]}$ yielded the trimetallic complexes *mer*-$\mathrm{[SnPh_2\{Fe(CO)_3[Si(OMe)_3](dppm{-}}$*P*$\mathrm{)\}_2]}$ and *mer,cis*-$\mathrm{[Fe(CO)_3(dppm)(SnClPh_2)_2]}$. The structure of the $\mathrm{CH_2Cl_2}$ solvate of the latter was determined by X-ray diffraction. Bridging by the dppm ligand was deduced from the ^1J(P–Sn) couplings detected by ^{31}P-{^{1}H} NMR spectroscopy. This result contrasts with the long P–Sn distance of 3.140 Å found in the crystal structure. This complex represents the first Fe–Sn complex containing a bridging dppm ligand. With $\mathrm{K[Fe(CO)_3\{Si(OMe)_3\}\{(Ph_2P)C_5H_4N\}]}$ the new bimetallic complexes *mer*-$\mathrm{[\{[(MeO)_3Si](OC)_3Fe[\mu{-}(Ph_2P)C_5H_4N]Zn(\mu{-}Cl)\}_2]}$ and *mer*-$\mathrm{[\{(MeO)_3Si\}(OC)_3Fe\{\mu{-}(Ph_2P)C_5H_4N\}MCl_2]}$ (M = Ga or In) have been prepared. The reactivity of the first towards donor ligands such as isocyanides or 4-methylpyridine was studied. It also reacts in non-polar solvents with an equivalent of $\mathrm{K[Fe(CO)_3(PPh_3)\{Si(OMe)_3\}]}$ to give the trimetallic chain complex $\mathrm{[Zn\{Fe(CO)_3[Si(OMe)_3][\mu{-}(Ph_2P)C_5H_4N]\}_2]}$ which transforms into an ionic species *mer*-$\mathrm{[\{(MeO)_3Si\}(OC)_3Fe\{\mu{-}(Ph_2P)C_5H_4N\}Zn][Fe(CO)_3\{Si(OMe)_3\}\{(Ph_2P)C_5H_4N\}]}$ in donor solvents like tetrahydrofuran. Complexes containing the cyanometalate $\mathrm{(C_5H_4Me)\ Mn(CO)_2(CN)}$ are also described.

Since the early work of the groups of Mays and Burlitch,[1] only few heterometallic chain complexes of Zn, Cd and Hg containing three different metals have been described. This may be due to the often-observed tendency of such complexes to undergo redistribution reactions and to form symmetric species, although there is no conclusive description of the factors governing such rearrangements.[2] As part of our recent interest in silicon-containing heterometallics, we have used anionic silyl complexes such as $\mathrm{[Fe(CO)_3(PR'_3)(SiR_3)]^-}$ (R = OMe or OEt, R′ = alkyl or aryl) in substitution reactions with metal halides to prepare such di- and tri-nuclear compounds with unsupported as well as ligand-bridged metal–metal bonds.[3] We have shown that subtle changes may influence the outcome of such reactions. Thus, the formation of a binuclear, halide-bridged Fe–Cd complex was observed exclusively when starting from $\mathrm{CdBr_2}$ whereas only trinuclear Fe–Cd–Fe chains were found in the case of $\mathrm{CdCl_2}$.[3h] In contrast, M–Hg–X complexes show less tendency to form halide-bridged species[3l] and less is known about complexes containing Zn. We have previously reported the formation of Fe–Si–O–M′ four-membered ring systems with the metals M′ = Ag, Rh, Pd or Pt.[3a–e] In order better to understand the conditions for the occurrence of this unusual μ-(alkoxysilyl) bridging mode, we wished to prepare bimetallic complexes with more oxophilic metals having an unsaturated co-ordination sphere. Following our studies on Cd-containing complexes[3f,h,i] we were interested in expanding this chemistry to Group 13 elements and we report here the rational synthesis and reactivity of new, stable heterometallic M–M′ (M = Fe, M′ = Ga or In) and M–M′–M″ arrays (M = Fe; M′ = Zn, Cd, Hg or In; M″ = Mo, W or NCMn) containing bridging ligands and alkoxysilyl groups.

Indium and gallium co-ordination compounds containing phosphine ligands have recently gained special interest for their widespread application as intermediates in the preparation of

---

* Part of Ph.D. Thesis of M. Strampfer, Université Louis Pasteur, 1993.

Supplementary data available: see Instructions for Authors, *J. Chem. Soc., Dalton Trans.*, 1994, Issue 1, pp. xxiii–xxviii.

the Group 13–Group 14 semiconductors.[4] On the other hand, heterometallic complexes containing direct metal–metal bond(s) between main-group elements and transition metals are attractive as potential precursors of new materials with particular properties.[5] This implies the availability of synthetic methods to prepare and stabilise such complexes. Since the early reports about compounds with transition metal–indium bonds,[6] little research has been done in this field. However there is a growing interest in the co-ordination chemistry and structural features of heterometallic indium[7] and gallium complexes.[8a–e] Finally we felt it interesting to extend this approach to the synthesis of Fe/Si/Sn complexes, knowing that the tin atom displays a great variety of co-ordination numbers and bonding modes.[8f,g]

The anionic iron silyl complexes $K[Fe(CO)_3\{Si(OMe)_3\}L]$ [L = PPh_3,[3e] **2a**, $Ph_2PCH_2PPh_2$ (dppm)[3e] **2b**, $Ph_2P(CH_2)_4PPh_2$ (dppb)[3e] **2c** or 2-$(Ph_2P)C_5H_4N$ **2d**[3h]] were prepared by deprotonation of the corresponding hydrido silyl complexes **1** with KH as previously described (Scheme 1). The phosphine ligand L was chosen in order to evaluate the influence of potential bridging donors on the properties of the bimetallic complexes which were expected to result from the reactions of the iron metalates with metal halides.

Results and Discussion

Complexes with Unsupported Metal–Metal Bonds.—When 1 equivalent of complex **2a** was treated with a slight excess of $InCl_3$ the new colourless complex **3** was formed in high yields. A similar reaction with $InBr_3$ gave the pale yellow complex **4**. On the other hand, **4** and yellow **5** were quantitatively obtained when **3** was stirred in CH_2Cl_2 with a slight excess of KBr or KI, respectively. Complexes **3**–**5** exhibit comparable spectroscopic properties. The characteristic ν(CO) absorption pattern of the *mer*-carbonyls on iron is slightly shifted to lower wavenumbers on going from **3** to **5**, consistent with the decreasing electronegativity of Cl to I. In all three cases no notable MeO→In interaction could be evidenced by ^1H NMR spectroscopy even at low temperature (190 K), where such an interaction should lead to chemically inequivalent methoxy groups with an intensity ratio of 2:1.[3] Characteristic stretches at 320, 254 and 250 cm^{-1} in the FIR region of **3** indicate a dimeric structure for this complex with terminal and bridging chlorides. In the dinuclear complex $[(Cl)RIn(\mu\text{-}Cl)_2InR(Cl)]$ (R = organic group) the bridging chlorides were observed at 190–250 cm^{-1} whereas the terminal ν(In–Cl) stretches are generally found between 280 and 330 cm^{-1}.[9] A similar structure is likely for **4** and **5**. This results in a four-co-ordinate tetrahedral indium centre, as found in other complexes of In^{III} of the type $[InX_3(PR_3)]$[10] or $[InM_2X(L)]$ which contain metal–metal bonds (L = base, M = Cr or Mo).[7e]

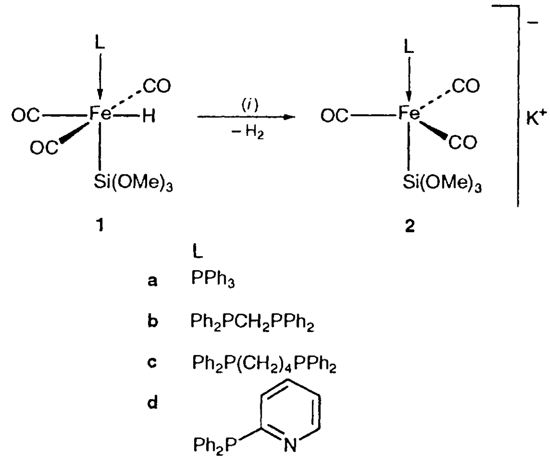

Scheme 1 (*i*) KH, tetrahydrofuran (thf)

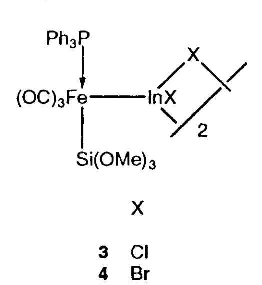

X
3 Cl
4 Br
5 I

These halide bridges are easily split by Lewis bases. The IR bands of complex **3** in thf are shifted towards lower wavenumbers when compared to those in CH_2Cl_2, consistent with co-ordination of thf to indium as a result of adduct formation or splitting of the chloride bridges which appears more likely in view of the spectroscopic similarities with **6** (see below) and of previous observations.[6b,7e] A similar behaviour is observed by IR spectroscopy [ν(CO) and ν(CN) region] when Bu^tNC is added to a CH_2Cl_2 solution of **3**. Complete conversion of **3** requires an excess of isocyanide, suggesting that an equilibrium is established. Unfortunately, no isocyanide-containing complex could be isolated pure. Reaction of **3** with triphenylphosphine oxide or with 4-methylpyridine (4Me-py) afforded **6** and **7**, respectively, but no reaction was observed by IR spectroscopy [ν(CO) and ν(CN) region] with MeCN, PPh_3 or $Ph_2PCH_2C(O)Ph$, although the latter was successfully used in related Fe–Cd complexes.[3f] Complexes **6** and **7** were characterised by usual analytical and spectroscopic methods. Their IR absorptions in CH_2Cl_2 are are very similar and again indicate a *mer* arrangement of the CO ligands.

A typical decrease of *ca.* 15 cm^{-1} was observed in the ν(CO) stretches of complexes **6** and **7** compared to their precursors. The ν(P–O) vibration of the indium-co-ordinated triphenylphosphine oxide in **6** is found at 1144 cm^{-1}, 43 wavenumbers lower than for the free phosphine oxide. The absorptions in the FIR region at 302 and 296 cm^{-1} are characteristic for terminal In–Cl groups.[9] The singlet resonance due to the $Si(OMe)_3$ group in the proton NMR spectrum of **6** is slightly broadened at room temperature. On decreasing the temperature coalescence is reached at 263 K and at 223 K two distinct resonances in a 2:1 ratio are observed, indicating a Fe–Si–O–In interaction ($\Delta G^\ddagger = 53.5 \pm 2$ kJ mol^{-1}) (see below).[*] For related Fe–Si–O–Pd interactions $\Delta G^\ddagger$ was found to be 65 ± 2 kJ mol^{-1}.[3c] The $^{31}P\text{-}\{^1H\}$ NMR spectrum displays two resonances at δ 56.1 (sharp) for the iron-bound phosphorus atom and at δ 35.7 (br) for the indium-bound phosphine oxide, shifted by 5 ppm compared to free triphenyl phosphine oxide (δ 29.3).[12] Interestingly, the intensity ratio of these two peaks is 1:5, indicating very different relaxation times for the two types of phosphorus atoms. By applying a relaxation delay of 3 s their integral intensities became equivalent.

The detailed geometry of complex **6** was established by single-crystal X-ray analysis. The structure is shown in Fig. 1 and

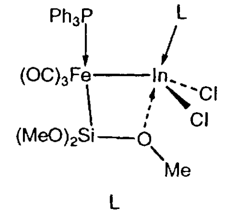

L
6 O=PPh3
7 4Me-py

---

[*] The $\Delta G^\ddagger$ values for exchange processes observed *via* NMR spectroscopy were calculated by using the Eyring equation.

selected bond distances and angles are given in Table 1. The iron and indium centres are linked by a metal–metal bond [*d*(Fe–In) = 2.600(1) Å] which falls within the range of values reported for the polynuclear complexes [{In[Fe(C_5H_5)(CO)$_2$]$_2$(μ-Cl)}$_2$] [*d*(Fe–In) = 2.553(1), 2.558(1) Å] and [InCl{Fe(C_5H_5)(CO)$_2$}$_2$-(PPhMe$_2$)] [*d*(Fe–In) = 2.582(1), 2.569(1) Å][7f] but is shorter than in **12** [*d*(Fe–In) = 2.680(1) Å] (see below) and considerably shorter than the sum of the covalent van der Waals radii of 2.71 Å.* The six-co-ordinated environment of the Fe atom is determined by the In atom, the phosphorus atom from the PPh$_3$ ligand, a Si atom from the Si(OMe)$_3$ ligand and the three carbon atoms from the terminal carbonyl groups. This environment is similar to that found in other complexes of the type *mer*-[FeM(CO)$_3$(PR$_3$){Si(OMe)$_3$}] (M = transition metal).[3] It may be viewed as distorted octahedral or as trigonal bipyramidal, when ignoring the Fe–In bond. This latter description is more consistent with a formal iron(0) d^8 centre. The C(1)–Fe–C(3) angle of 159.9(4)° is probably the result of the stereoelectronic requirement of the iron centre rather than of bonding interactions between these carbonyl groups and the indium centre.

Table 1 Selected bond distances (Å) and angles (°) in *mer*-[(Ph$_3$P)-(OC)$_3$Fe{μ-Si(OMe)$_2$(OMe)}InCl$_2$(O=PPh$_3$)] **6**

In–Cl(1)	2.418(2)	Si–O(4)	1.608(7)
In–Cl(2)	2.391(2)	Si–O(5)	1.639(7)
In–Fe	2.600(1)	Si–O(6)	1.642(6)
In–O(6)	2.584(6)	O(4)–C(4)	1.39(1)
In–O(7)	2.221(5)	O(6)–C(6)	1.41(1)
Fe–C(1)	1.775(9)	P(1)–C(7)	1.845(8)
Fe–C(2)	1.749(9)	P(1)–C(13)	1.833(8)
Fe–C(3)	1.792(9)	P(1)–C(19)	1.845(8)
Fe–Si	2.311(2)	O(5)–C(5)	1.37(1)
Fe–P(1)	2.278(2)	P(2)–O(7)	1.501(5)
C(1)–O(1)	1.148(9)	P(2)–C(25)	1.801(9)
C(2)–O(2)	1.148(9)	P(2)–C(31)	1.818(9)
C(3)–O(3)	1.14(1)	P(2)–C(37)	1.811(7)
Cl(1)–In–Cl(2)	108.4(1)	C(1)–Fe–C(3)	159.9(4)
Cl(1)–In–Fe	123.0(1)	C(2)–Fe–C(3)	98.2(4)
Cl(1)–In–O(6)	80.5(2)	Fe–C(1)–O(1)	178.4(7)
Cl(1)–In–O(7)	90.3(1)	Fe–C(2)–O(2)	179.0(7)
Cl(2)–In–Fe	121.4(1)	Fe–C(3)–O(3)	178.0(7)
Cl(2)–In–O(6)	88.3(2)	O(4)–Si–O(5)	109.1(4)
Cl(2)–In–O(7)	93.1(2)	O(4)–Si–O(6)	112.0(4)
Fe–In–O(6)	75.4(1)	O(5)–Si–O(6)	100.9(4)
Fe–In–O(7)	111.5(1)	Si–O(4)–C(4)	130.9(9)
O(6)–In–O(7)	170.7(2)	Si–O(5)–C(5)	132.5(8)
C(1)–Fe–C(2)	99.2(4)	Si–O(6)–C(6)	128.8(7)
C(1)–Fe–Si	87.7(3)	Si–Fe–In	81.1(7)
C(1)–Fe–P(1)	94.3(2)	P(1)–Fe–In	103.0(1)
C(2)–Fe–Si	82.7(3)	In–O(7)–P(2)	147.6(3)
C(2)–Fe–P(1)	93.1(3)	O(7)–P(2)–C(31)	113.2(4)
C(3)–Fe–Si	84.7(2)	O(7)–P(2)–C(37)	109.9(3)
C(3)–Fe–P(1)	94.6(2)	O(7)–P(2)–C(25)	113.6(4)
Si–Fe–P(1)	175.7(1)		

Numbers in parentheses are estimated standard deviations (e.s.d.s) in the least significant digits.

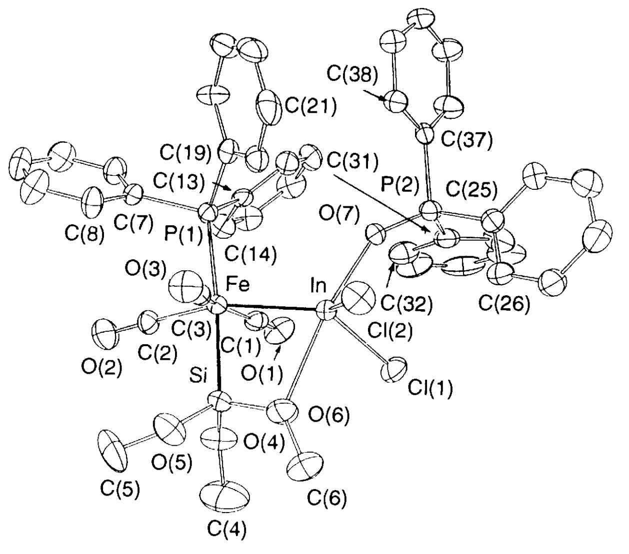

Fig. 1 Structure of *mer*-[(Ph$_3$P)(OC)$_3$Fe{μ-Si(OMe)$_2$(OMe)}InCl$_2$-(O=PPh$_3$)] **6** showing the atom numbering scheme. Ellipsoids enclose 50% of the electron density

The distorted trigonal-bipyramidal environment around the indium atom involves the Fe atom, two chlorine atoms, the oxygen atom from the phosphine oxide ligand and one oxygen atom from the SiOMe group [O(6)–In–O(7) 170.7(2)°]. The distance In–O(6) of 2.584(6) Å can be compared with those in adducts with oxygen-donor ligands like ethers, which fall in the range 2.371(5)–2.67(2) Å.[15]

This rare co-ordination mode of the alkoxysilyl group established for the solid-state structure as well as in solution (by ^{1}H NMR spectroscopy, see above) is comparable to the situation found in related complexes like *mer*-[(OC)$_3$Fe{(μ-Si(OMe)$_2$(OMe)}(μ-dppm)PdCl] **A** [*d*(O–Pd) = 2.100(4) Å],[3a] *mer*-[(OC)$_3$Fe{μ-Si(OMe)$_2$(OMe)}(μ-dppm)Rh(CO)] **B** [*d*(O–Rh) = 2.167(3) Å],[3d] *mer*-[{(OC)$_3$Fe[μ-Si(OMe)$_2$-(OMe)][μ-Ph$_2$PCH$_2$C(O)Ph]Cd(μ-Cl)}$_2$] **C** [*d*(O–Cd) = 2.515(5) Å][3i] or [Cd{Fe(CO)$_3$[μ-Si(OMe)$_2$(OMe)][{Ph$_2$-PCH$_2$C(O)C$_5$H$_4$]Fe(C$_5$H$_5$)}]}$_2$] **D** [*d*(O–Cd) = 2.541(5) Å].[3i]

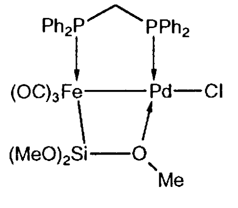

A

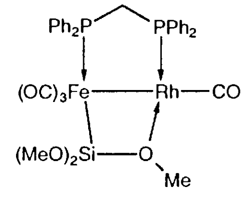

B

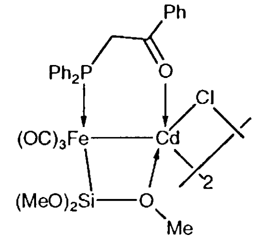

C

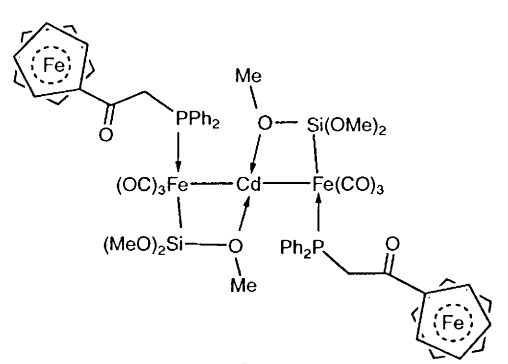

D

---

* Derived as described[7f] from a literature value of 1.44 Å for In^{III} and a value for Fe derived from the bond length in [Fe$_2$(CO)$_4$(C$_5$H$_5$)$_2$] of 2.543(2) Å.[14]

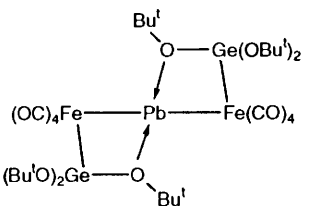

E

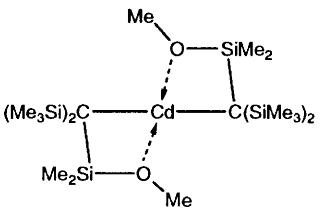

F

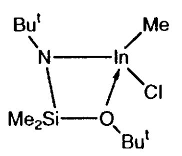

G

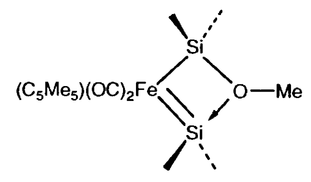

H

Considering that the atomic radius[16] of In is 0.027 Å longer than that of Cd, the In–O(6) [2.584(6) Å] distance compares with the corresponding (O–Cd) distances (see above) found in complex **C** or **D**. However, these distances are much longer than those found in related Fe–Pd and Fe–Rh complexes **A** and **B** since the difference in atomic radii between these metals does not exceed 0.19 Å [*r*(In) – *r*(Pd) = 0.157; *r*(In) – *r*(Rh) = 0.188 Å]. This results in bonding distances between harder metals such as Cd or In and the oxygen donor of the methoxy group being much longer than in complexes where this oxygen is co-ordinated to softer metals like Rh or Pd. It is interesting that somewhat related Fe–Si–O–(element) four-membered rings have been found in Pb{Fe[μ-Ge(OBu^t)$_2$(OBu^t)]}$_2$ **E** [*d*(O–Pb) = 2.64(1) Å],[17a] [Cd{C(SiMe$_3$)$_2$[μ-SiMe$_2$(OMe)]}$_2$ **F** [*d*(O–Cd) = 3.09 Å],[17b] in aminoalkoxysilyl complexes of type **G** [17c] and in methoxy-stabilised bis(silylene)iron complexes **H**.[17d]

Comparison of the structures of complexes **3** and **6** suggests that co-ordination of a donor molecule such as O=PPh$_3$ promotes the Fe–Si–O→In interactions by favouring a change in the co-ordination sphere around indium from tetrahedral (in **3**) to distorted trigonal bipyramidal. The O(7)–In distance of the phosphine oxide [2.221(5) Å] in **6** is comparable to that in the recently described complexes [InCl$_3$(O=PR$_3$)$_n$] (*n* = 2 or 3) where the O–In distances are between 2.196(7) and 2.231(4) Å.[18] The P–O distance of 1.501(5) Å is, as generally observed, only little influenced by the nature of the metal to which it is co-ordinated (P–O distances in P–O–M complexes are reviewed in ref. 19). The shorter P–O distance of 1.483(2) Å in unco-ordinated O=PPh$_3$ [20] is consistent with the higher ν(P–O) stretch in its IR spectrum compared with those of co-ordinated phosphine oxides. The angle P(2)–O(7)–In [147.9(3)°] falls in the normal range.[18,19] Angles in M–O–P (M = Group 13 element) arrays can adopt linear as well as bent geometries which have been discussed in terms of σ (linear, end-on) and π (bent, side-on) bondings.[19] The angle is however strongly influenced by steric factors and even packing forces in the crystal, due to the small energy difference between the bent and linear forms. The torsion angle P(1)–Fe–In–O(7) is 15.8(3)°.

The reaction of 2 equivalents of complex **2a** with InCl$_3$ or of 1 equivalent of **2a** with **3** gave in high yields the new yellow complex *mer*-[InCl{Fe(CO)$_3$(PPh$_3$)[μ-Si(OMe)$_2$(OMe)]}$_2$] **8**. Its FIR spectrum contains a strong ν(In–Cl) absorption at 286 cm^{-1}, suggesting a terminal chlorine atom and therefore a monomeric species.[9] The ^{31}P-{^{1}H} NMR spectrum contains a resonance at δ 57.4 due to the iron-bound PPh$_3$ ligand. Only a singlet resonance is observed in the room-temperature ^{1}H NMR spectrum for the Si(OMe)$_3$ protons. On decreasing the temperature this signal broadens to give three distinct singlets at 2.89, 3.56 and 3.65 in a 1 : 1 : 1 ratio at 183 K (Fig. 2). This phenomenon is reversible when raising the temperature and corresponds to a freezing of the Si(OMe)$_3$ motions. The more downfield resonance most likely corresponds to a methoxy group interacting with the indium centre whereas the two very close singlet resonances correspond to the other two methoxy groups which are magnetically inequivalent owing to the co-ordination geometry of the In atom. The latter two resonances coalesce at 203 K to give a singlet which in turn coalesces with the resonance at δ 2.89 around 213 K. These two coalescences correspond to only one dynamic phenomenon characterised by $\Delta G^\ddagger$ = 42 ± 2 kJ mol^{-1} which represents the formation/rupture of the μ-SiOMe bridge.[11] A related splitting of the Si(OMe)$_3$ resonance into three singlets has been observed previously in a low-symmetry Fe–Rh complex[3d] for which the $\Delta G^\ddagger$ value was calculated to be 60 ± 2 kJ mol^{-1}. These data suggest the structure shown for **8** with a pentagonal-bipyramidal indium centre including two Fe–Si–O→In interactions, an approximate C_2 symmetry being also consistent with the number of ν(CO) bands observed. In solution, the methoxy groups of each Si(OMe)$_3$ ligand rapidly exchange by rotation about the Fe–Si bond and give rise to the singlet resonance observed at room temperature.

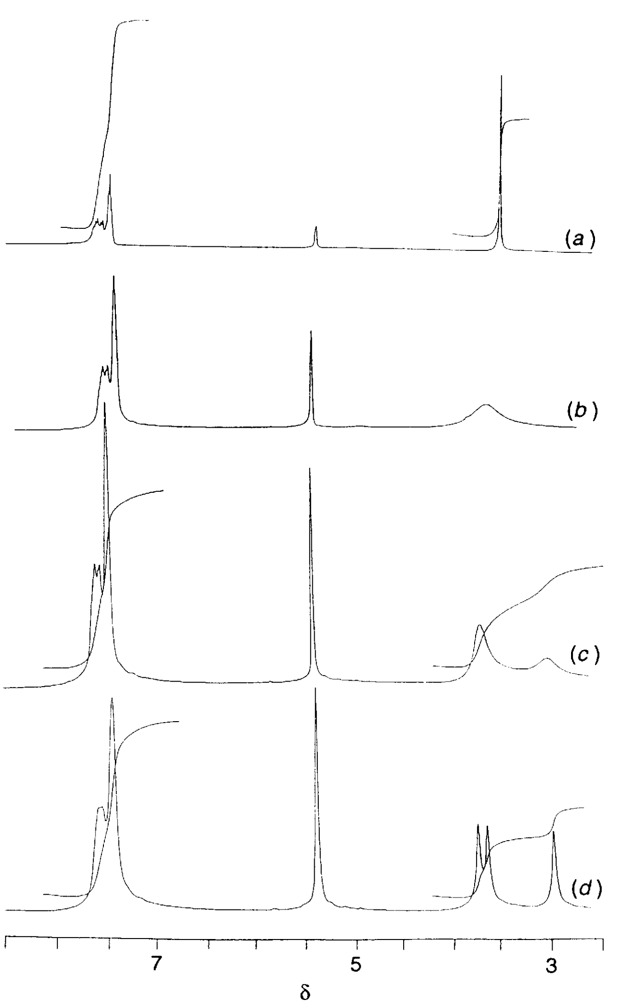

Fig. 2 Variable-temperature ^{1}H NMR spectrum of the complex *mer*-[InCl{Fe(CO)$_3$(PPh$_3$)[μ-Si(OMe)$_2$(OMe)]}$_2$] **8** at (*a*) 273, (*b*) 213, (*c*) 203 and (*d*) 183 K in CD$_2$Cl$_2$

Reaction of complex **8** with 1 equivalent of O=PPh$_3$ gave the new colourless complex *mer*-[InCl(O=PPh$_3$){Fe(CO)$_3$-(PPh$_3$)[Si(OMe)$_3$]}$_2$] **9** the suggested geometry of which (Scheme 2) is based on spectroscopic data. The IR spectrum in the carbonyl region exhibits three distinct absorptions at 2028, 1981 and 1951 cm^{-1}. In the FIR region a strong broad absorption at *ca.* 290 cm^{-1} is detected which is characteristic for

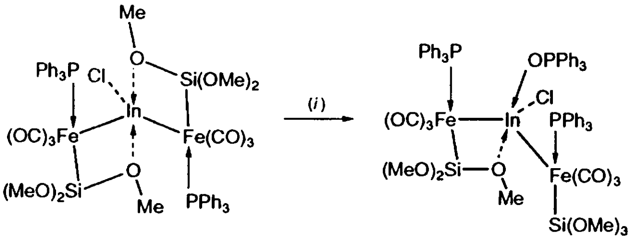

8 9

Scheme 2 (*i*) O=PPh$_3$, CH$_2$Cl$_2$

terminal ν(In–Cl) stretches.[9] The singlet resonance of the Si(OMe)$_3$ protons at δ 3.57 is broad at room temperature but resolves at 223 K into two distinct signals in a 5:1 ratio, consistent with only one methoxy group involved in a Fe–Si–O→In interaction. Coalescence is reached at 266 K, corresponding to a $\Delta G^\ddagger$ of 54 ± 2 kJ mol^{-1}.[11] The ^{31}P-{^{1}H} NMR spectrum shows two signals, one at δ 57.4 due to the Fe-bound phosphorus atom and the other at δ 28.1 due to the indium-bound phosphine oxide. When no relaxation delay was applied, the intensity ratio of the two phosphorus resonances (2:5) did not correspond to the expected ratio, as observed before for **6**. The ν(P=O) frequency of 1144 cm^{-1} found by IR spectroscopy is identical to that for **6**. It is worth mentioning that the infrared spectra of **8** and **9** display in the fingerprint region between 400 and 1500 cm^{-1} a pattern very similar to that of complexes **3** and **6**, respectively.

Reaction of complex **2a** with GaCl$_3$ in thf did not lead to a complex similar to **3**, but instead the hydride **1a** was formed quantitatively. A similar result was observed when K[Fe(CO)$_3$(PMePh$_2$){Si(OMe)$_3$}] (prepared in a manner similar to **2a**), K[Fe(CO)$_3${Ph$_2$PCH$_2$C(O)Ph}{Si(OMe)$_3$}][3e] or K[Fe(CO)$_3${Ph$_2$P(CH$_2$)$_2$CN}{Si(OMe)$_3$}][3i] were treated with GaCl$_3$ in thf. A comparable phenomenon has previously been reported when Na[Fe(CO)$_3$(PPh$_3$)(SiMePh$_2$)] was treated with ZnCl$_2$. Formation of [FeH(CO)$_3$(PPh$_3$)(SiMePh$_2$)] was explained by the initial formation of a bimetallic species which rapidly decomposed with cleavage of the metal–metal bond.[21] It has also been observed that the polar metal–metal bond of [(OC)$_4$Co–GaR$_2$(thf)] (R = CH$_2$Bu^t or CH$_2$SiMe$_3$) is cleaved by water to yield the cobalt hydride [CoH(CO)$_4$] and alkylgallium hydroxides.[8c]

Attempts to form complexes similar to **3** by reaction of **2a** with TlCl$_3$ were unsuccessful, instead redox reactions occurred with precipitation of TlCl (see below).

Complexes with Group 13 *Elements containing dppm Bridges.*—In contrast to the reactions of GaCl$_3$ with complex **2a** or with metalates carrying a weak pendant donor (see above), the reaction of **2b** with an excess of GaCl$_3$ in thf gave the stable pale yellow complex *mer*-[{(MeO)$_3$Si}(OC)$_3$Fe(μ-dppm)GaCl$_2$] **10** in high yields. In this case no metal–metal bond cleavage or formation of the hydride **1b** was observed. This represents an interesting demonstration of the stabilising effect provided by assembling ligands in the synthesis of gallium–transition metal complexes, also found with [(OC)$_3$Co(μ-dmpm)GaR$_2$] (dmpm = Me$_2$PCH$_2$PMe$_2$; R = CH$_2$Bu^t or CH$_2$SiMe$_3$).[8c] Complex **10** was characterised by usual analytical and spectroscopic methods. In the IR spectrum three characteristic absorptions for carbonyl groups in a *mer* arrangement around the iron centre are observed at 2030, 1972 and 1959 cm^{-1}. Two strong bands in the FIR spectrum at 370 and 340 cm^{-1} can be attributed to terminal ν(Ga–Cl) stretches.[9] The ^{31}P-{^{1}H} NMR spectrum shows a typical AX pattern with two doublets at δ 62.5 and −15.7 due to the iron- and gallium-bound phosphorus atoms of the dppm ligand, respectively, with a ^{2+3}J(P–P) coupling constant of 125 Hz. In the ^{1}H NMR spectrum no line broadening of the singlet resonance due to the Si(OMe)$_3$ protons was observed even at 180 K, ruling out any significant Fe–Si–O→Ga interaction. Similarly, the reaction of **2b** with

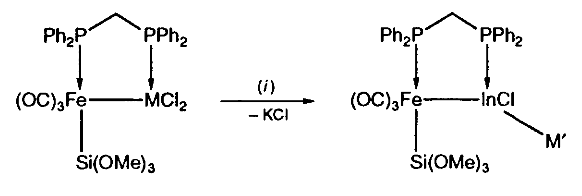

M
10 Ga
11 In

M′
12 Mo(C$_5$H$_4$Me)(CO)$_3$
13 W(C$_5$H$_5$)(CO)$_3$

Scheme 3 Na[Mo(C$_5$H$_4$Me)(CO)$_3$] or Na[W(C$_5$H$_5$)(CO)$_3$], thf

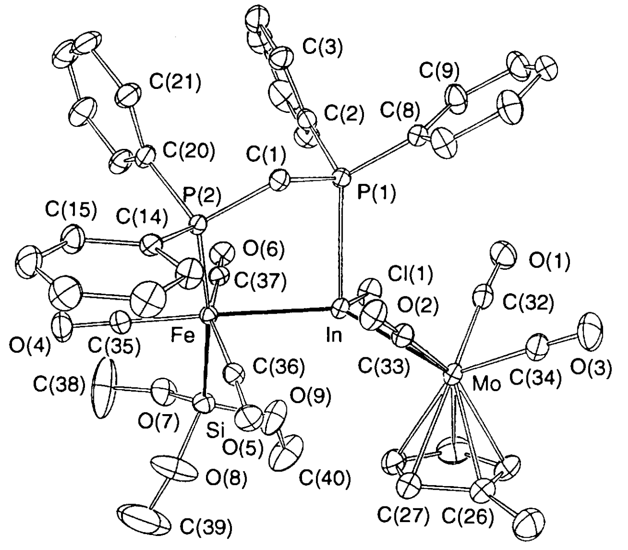

Fig. 3 Structure of *mer*-[{(MeO)$_3$Si}(OC)$_3$Fe(μ-dppm)InCl{Mo(C$_5$H$_4$Me)(CO)$_3$}] **12** showing the atom numbering scheme. Other details as in Fig. 1

InCl$_3$ gave colourless *mer* [{MeO)$_3$Si}(OC)$_3$Fe(μ-dppm)InCl$_2$] **11** in high yields. Its spectroscopic data are very similar to those of **10**. The absorption due to the iron-bound carbonyl groups are 9 cm^{-1} lower for **11** compared to **10**, due to a more polar Fe(δ$^-$)–In(δ$^+$) bond. We propose the structures illustrated for both **10** and **11**, with four-co-ordinate indium and gallium centres and direct iron–metal bonds.

Reaction of complex **11** with a slight excess of Na[Mo(C$_5$H$_4$Me)(CO)$_3$] or Na[W(C$_5$H$_5$)(CO)$_3$] in thf gave the new complexes **12** and **13** in high yields (Scheme 3). Use of an excess of [W(C$_5$H$_5$)(CO)$_3$]$^-$ led to liberation of some [Fe(CO)$_3$(dppm-*P*){Si(OMe)$_3$}]$^-$(^{31}P-{^{1}H} NMR evidence) and probably of [InCl(thf){Mo(C$_5$H$_5$)(CO)$_3$}$_2$],[6a,7e] although the latter was not isolated. The IR spectrum of **12** contains absorptions at 1980, 1917 and 1861 cm^{-1} corresponding to the molybdenum carbonyls at 2011, 1950 and 1944 cm^{-1} due to the *mer*-Fe(CO)$_3$ moiety, the latter absorptions being partly masked by the former. A similar pattern is found for **13**, the absorptions of the tungsten carbonyls being shifted towards lower wavenumbers by 5 cm^{-1}. In the FIR spectrum a strong absorption is detected at 261 cm^{-1} which is characteristic for a terminal ν(In–Cl) stretch although it is situated at the lower end of the usual range.[9] The ^{31}P-{^{1}H} NMR spectrum shows an AX pattern similar to that found for **10** and **11** with a ^{2+3}J(P–P) coupling of 122 Hz for **12** and 120 Hz for **13**. As in **10** and **11**, no Fe–Si–O→In interaction could be detected in the ^{1}H NMR spectra of **12** and **13** down to 190 K. No rearrangement or symmetrisation reactions were observed with pure samples. A single-crystal X-ray analysis was performed on **12** in order to establish the detailed molecular geometry of a representative member of this family of complexes. The structure is shown in Fig. 3 and selected bond distances and angles are given in Table 2.

The iron centre is co-ordinated by six ligands: three *mer*-

Table 2 Selected bond distances (Å) and angles (°) in *mer*-[{(MeO)$_3$Si(OC)$_3$Fe(μ-dppm)InCl{Mo(C$_5$H$_4$Me)(CO)$_3$}] **12**

In–P(1)	2.778(1)	P(2)–Fe	2.253(1)	C(34)–O(3)	1.155(6)	Fe–Si	2.307(1)
In–Mo	2.843(1)	Mo–C(34)	1.964(5)	C(29)–C(30)	1.381(9)	Fe–C(37)	1.792(4)
In–C(32)	2.895(5)	Mo–C(33)	1.959(5)	O(9)–C(40)	1.431(7)	Fe–C(36)	1.779(4)
In–Fe	2.680(1)	Mo–C(32)	1.981(6)	O(8)–C(39)	1.35(1)	Fe–C(35)	1.764(4)
In–C(37)	2.877(4)	C(26)–C(29)	2.25(1)	O(7)–C(38)	1.323(9)	Mo–C(30)	2.308(5)
In–Cl(1)	2.453(1)	C(26)–C(30)	1.385(9)	Si–O(9)	1.635(4)	Mo–C(29)	2.318(6)
P(1)–C(1)	1.834(4)	C(26)–C(31)	1.55(1)	Si–O(8)	1.597(4)	Mo–C(28)	2.322(5)
P(1)–C(2)	1.814(4)	C(27)–C(28)	1.372(9)	Si–O(7)	1.630(4)	Mo–C(27)	2.314(6)
P(1)–C(8)	1.831(4)	C(28)–C(29)	1.42(1)	C(37)–O(6)	1.130(5)	Mo–C(26)	2.316(6)
P(2)–C(1)	1.836(4)	C(32)–O(1)	1.143(6)	C(36)–O(5)	1.145(5)	In–C(36)	2.951(5)
P(1)–C(14)	1.837(4)	C(33)–O(2)	1.148(6)	C(35)–O(4)	1.153(5)	In–O(9)	3.159(5)
P(2)–C(20)	1.821(4)						
P(1)–In–Mo	107.6(1)	C(37)–In–Cl(1)	80.15(9)	C(1)–P(1)–C(8)	103.4(2)	P(2)–Fe–C(37)	99.9(1)
P(1)–In–C(32)	83.9(1)	C(32)–Mo–C(33)	103.7(2)	C(2)–P(1)–C(8)	105.4(2)	Fe–C(35)–O(4)	179.6(7)
P(1)–In–Fe	90.04(2)	C(32)–Mo–C(34)	79.3(2)	C(1)–P(2)–C(14)	102.9(2)	Fe–C(37)–O(6)	177.1(4)
P(1)–In–C(37)	84.14(8)	C(33)–Mo–C(34)	80.5(2)	C(1)–P(2)–C(20)	103.2(2)	Fe–C(36)–O(5)	177.5(4)
P(1)–In–Cl(1)	99.59(4)	C(35)–Fe–Si	84.2(2)	C(1)–P(2)–Fe	118.3(1)	O(7)–Si–O(8)	106.8(2)
Mo–In–C(32)	40.4(1)	C(36)–Fe–Si	84.1(1)	P(1)–C(8)–C(9)	118.2(4)	O(8)–Si–O(9)	109.6(3)
Mo–In–Fe	131.6(1)	C(37)–Fe–Si	82.6(1)	P(1)–C(8)–C(13)	122.9(3)	O(7)–Si–O(9)	103.7(2)
Mo–In–C(37)	165.4(1)	Fe–Si–O(7)	115.8(2)	P(2)–Fe–Si	171.8(1)	Mo–C(32)–O(1)	175.5(5)
Mo–In–Cl(1)	105.6(1)	Fe–Si–O(8)	111.7(2)	C(35)–Fe–C(36)	101.6(2)	Mo–C(33)–O(2)	175.2(4)
C(32)–In–Fe	165.9(1)	Fe–Si–O(9)	109.0(2)	C(35)–Fe–C(37)	100.1(2)	Mo–C(34)–O(3)	178.8(5)
C(32)–In–C(37)	153.0(1)	C(14)–P(2)–C(20)	102.3(2)	C(36)–Fe–C(37)	153.3(2)	Si–O(7)–C(38)	131.8(5)
C(32)–In–Cl(1)	78.1(1)	C(14)–P(2)–Fe	110.8(1)	P(2)–Fe–C(35)	87.7(2)	Si–O(8)–C(39)	132.1(8)
Fe–In–C(37)	37.42(9)	C(20)–P(2)–Fe	117.4(2)	P(2)–Fe–C(36)	96.4(1)	Si–O(9)–C(40)	126.2(5)
Fe–In–Cl(1)	115.6(1)	C(1)–P(1)–C(2)	105.6(2)				

carbonyls, the Si(OMe)$_3$ group, one phosphorus atom of the dppm ligand and the indium atom. The separation of 2.877(4) Å between C(37) and In is unlikely to represent a significant bonding interaction in view of the almost linear Fe–C(37)–O(6) angle [177.1(4)°]. The iron centre may be viewed as having a distorted trigonal-bipyramidal co-ordination, when ignoring the Fe–In bond. We have encountered this type of structure in several Fe–M complexes and this appears to be a general feature (see discussion for **6**). The co-ordination sphere of the indium centre is tetrahedral, formed by one phosphorus atom of the bridging dppm ligand, the metal–metal bonds to iron and to molybdenum and one chlorine atom. The In–P(1) distance in **12** of 2.778(1) Å is at the upper limit of the usual range of In–P distances (2.576–2.810 Å).[10,22] The molybdenum atom exhibits a four-legged piano-stool geometry. The distances In–C(32) [2.895(5) Å] and In–O(9) [3.159(5) Å] are too long to represent significant bonding interactions. The torsion angle P(1)–In–Fe–P(2) is 18.59(9)°. To the best of our knowledge **12** is the first characterised transition-metal indium complex containing a bridging dppm ligand. Furthermore, the only example known to us of an indium complex containing two different transition metals is [(OC)$_5$MnIn{μ-Fe(CO)$_4$}$_2$InMn(CO)$_5$].[23]

No reaction was observed when donor ligands (N or P donors) were added to complexes **10**–**13**, ruling out the presence of any dimeric, halide-bridged species in solution. Attempts to form cationic complexes by chloride abstraction with TlPF$_6$ or Ag(O$_2$CMe) in the presence of electron-donor ligands were unsuccessful.

Attempts to prepare complexes comparable to **10** and **11** with TlCl$_3$ and **2b** were unsuccessful: a redox reaction with precipitation of insoluble TlCl occurred, similar to the one observed with **2a**. In contrast, the stable complex [{Si(OMe)$_3$}(OC)$_3$Fe(μ-dppm)Tl(C$_6$F$_5$)$_2$] has been obtained in good yields from **2b** and [TlBr(C$_6$F$_5$)$_2$].[3f]

A Fe–Cd–Mo trimetallic complex [{(MeO)$_3$Si}(OC)$_3$Fe(μ-dppm)Cd{Mo(C$_5$H$_4$Me)(CO)$_3$}] **14**, comparable to **12** and **13**, was synthesised from the bimetallic complex *mer*-[{[(MeO)$_3$Si](OC)$_3$Fe(μ-dppm)Cd(μ-Cl)}$_2$][3f] and 1 equivalent of Na[Mo(C$_5$H$_4$Me)(CO)$_3$] (Scheme 4). The same product was obtained when [BrCdMo(C$_5$H$_5$)(CO)$_3$][1b] was treated with 1 equivalent of **2b**. Complex **14** was characterised by IR and ^{31}P-{^{1}H} NMR spectroscopy. Its IR spectrum shows two sets of absorptions, one at 1983, 1919 and 1899 cm^{-1} corresponding to the ν(CO) stretches of the meridional carbonyls bound to iron, and the other at 1955, 1871 and 1836 cm^{-1}, corresponding to the three carbonyls of the distorted four-legged piano-stool (C$_5$H$_4$Me)Mo(CO)$_3$ fragment. In the ^{31}P-{^{1}H} NMR spectrum two doublet resonances are observed at δ 64.3 for the iron-bound phosphorus atom and at δ −15.4 for the cadmium-bound phosphorus atom of the dppm ligand, with ^{2+3}J(P–P) of 113 Hz. In addition the iron- and cadmium-bound phosphorus atoms are coupled to ^{111,113}Cd with ^{2+3}J(P–Cd) of 61 Hz and ^1J(P–Cd) of 398 Hz, respectively. The ^1J(P–Cd) coupling constant is smaller than the usual values (*ca.* 1200 Hz).[23] This may suggest a relatively weak Cd-bound phosphorus atom resulting in a limited stabilising effect of the bridging ligand on the Fe–Cd bond. This is supported by the observation that **14** slowly rearranges in solution, yielding the symmetric product [Cd{Fe(CO)$_3$[Si(OMe)$_3$](μ-dppm)}$_2$] (^{31}P-{^{1}H} monitoring).[3i] The chemical shift of the Cd-bound phosphorus atom is close to the value found for the structurally characterised *mer*-[{[(MeO)$_3$Si](OC)$_3$Fe(μ-dppm)Cd(μ-Cl)}$_2$][3f] for which, however, no ^1J(Cd–P) coupling was detected.

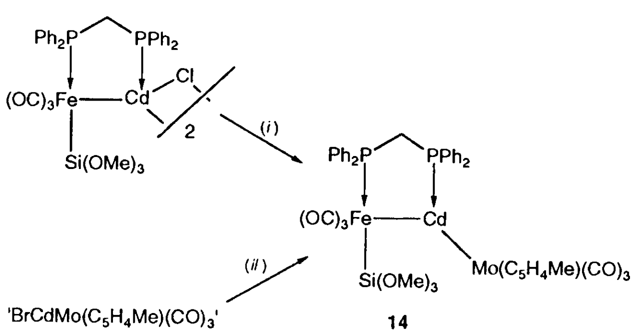

Scheme 4 (*i*) Na[Mo(C$_5$H$_4$Me)(CO)$_3$]; (*ii*) **2b**

dppb-Bridged Fe–In *Complex.*—The reaction of 1 equivalent of complex **2c** with InCl$_3$ afforded the colourless complex **15** in high yields. Characteristic absorptions are observed in its IR spectrum at 2023mw, 1972 (sh) and 1955vs cm^{-1} which indicate a meriodional arrangement of the iron carbonyls. The FIR

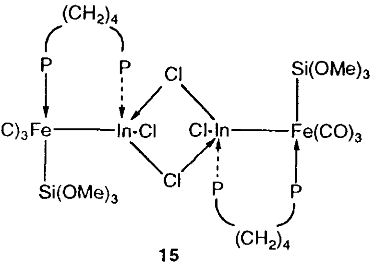

15

spectrum contains a very broad absorption between 330 and 250 cm^{-1} possibly indicating bridging and terminal chlorides.[9] Two broad resonances are observed in the ^{31}P-{^{1}H} NMR spectrum in thf at *ca.* δ 49 for the iron-bound phosphorus and at *ca.* δ −16 for the indium-bound phosphorus atom. For comparison, the resonance of the unco-ordinated P atom in [FeH(CO)$_3${Si(OMe)$_3$}(dppb-*P*)] is observed at δ −17.4,[3e] a value suggesting a phosphorus atom only loosely bound to indium in **15**. Decreasing the temperature of a CH_2Cl_2 solution of the complex leads to several distinct signals for the Fe-bound phosphorus atom which are probably due to the presence of different isomers in solution.[3e] The ^{1}H NMR spectrum shows a sharp singlet resonance at δ 3.49 corresponding to the Si(OMe)$_3$ groups and some unresolved resonances between δ 1.0 and 2.5 corresponding to the methylene protons of the dppb ligand. Addition of 1 equivalent of 4Me-py leads to co-ordination of the N-donor ligand (IR band at 1627 cm^{-1} for indium-bound 4Me-py and 1607 cm^{-1} for the unco-ordinated ligand). The indium-bound phosphine is most probably displaced by the N-donor ligand. The different potential donor groups present in the complex, *e.g.* the chloride ligands (bridges), the dppb ligand and the Si(OMe)$_3$ groups, may compete with each other, which could explain the spectroscopy of **15**. Caution must be exercised since solution and solid-state structures need not be identical. We suggest for **15** the structure illustrated which is comparable to that of *mer*-[{[(MeO)$_3$Si](OC)$_3$Fe(μ-Ph$_2$PCH$_2$CH$_2$C≡N)-In(μ-Cl)Cl}$_2$][3i] for which a bridging phosphinonitrile ligand was considered.

dppm-Containing Fe–Sn *Complex*.—We felt it interesting to see whether the stabilising effect of a bridging dppm ligand would lead to mixed Fe/Si/Sn complexes. A five-co-ordinated tin centre could result from nucleophilic attack of **2b** with a tin(IV) halide. Thus, reaction of 1 equivalent of **2b** with SnCl$_2$Ph$_2$ in thf was monitored by IR and ^{31}P-{^{1}H} NMR spectroscopy (Scheme 5). The first reaction product *mer*-[SnPh$_2${Fe(CO)$_3$[Si(OMe)$_3$](dppm-*P*)}$_2$] **16** displays typical IR bands at 2044, 2003 and 1970 cm^{-1} for the three *mer*-carbonyl ligands on iron. Four different doublets are observed in the ^{31}P-{^{1}H} NMR spectrum, two corresponding to the iron-bound phosphorus atoms at δ 48.0 and 42.7 with coupling to the ^{117,119}Sn isotopes of ^{2}J(P–Sn) of *ca.* 135 Hz; the other two doublets at δ −24.9 and −27.2 display ^{2}J(P–P) 58 and 55 Hz. A pendant PPh$_2$ group would resonate at *ca.* δ −23 and therefore the latter values would be consistent with weakly tin-co-ordinated phosphorus atoms. However, no ^{1}J(P–^{117,119}Sn) coupling was observed for the latter resonances. This suggestion is supported by the crystal structure determination of *mer,cis*-[Fe(CO)$_3$(dppm-*P*)(SnClPh$_2$)$_2$] **17** (see below). The ^{1}H NMR spectrum of **16** shows two different sharp singlet resonances for the Si(OMe)$_3$ group in a 1 : 1 ratio. After prolonged stirring of the reaction mixture the solution turns yellow, and formation of a 1 : 1 mixture of **16** and of a new product **17** is observed by ^{31}P-{^{1}H} NMR spectroscopy. This mixture could be separated by fractional crystallisation. Whereas **16** is slightly soluble in thf and forms a colourless powder, **17** is more soluble and tends to form yellow crystals. The IR spectrum of **17** exhibits the typical pattern for three carbonyl groups on iron in a *mer* arrangement. The ^{1}H NMR spectrum contains a doublet resonance for the methylene protons of the dppm ligand but no resonance for the Si(OMe)$_3$ protons could be observed, which indicated the loss of this group.

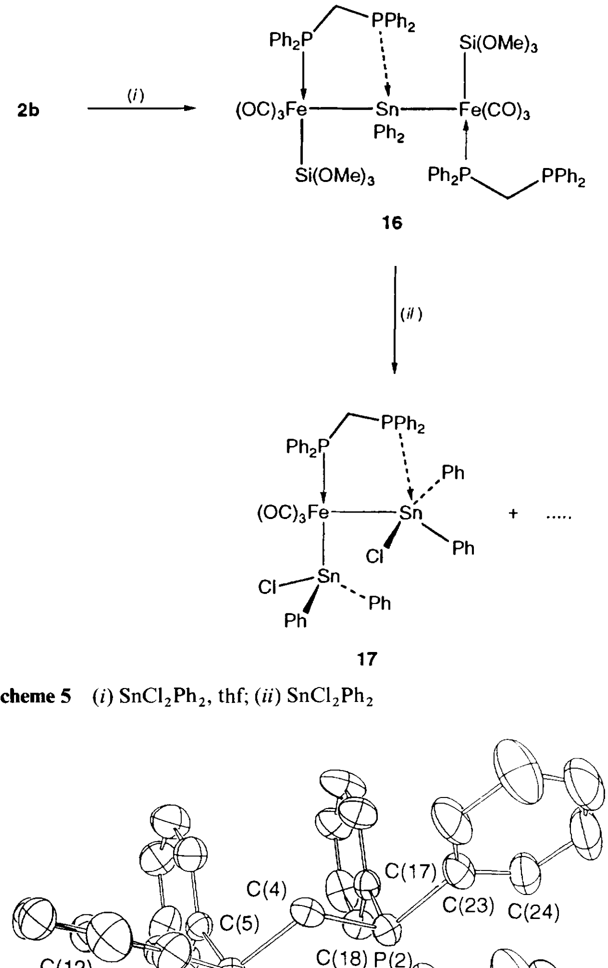

Scheme 5 (*i*) SnCl$_2$Ph$_2$, thf; (*ii*) SnCl$_2$Ph$_2$

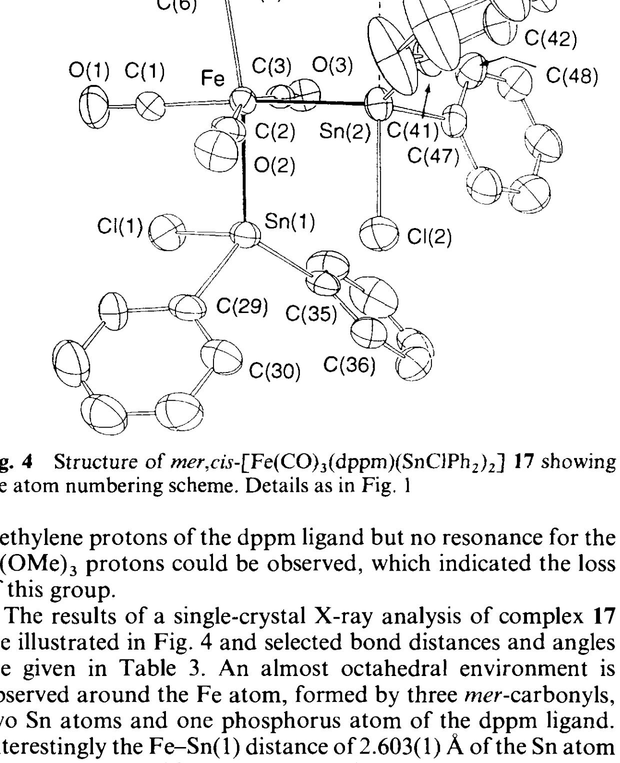

Fig. 4 Structure of *mer,cis*-[Fe(CO)$_3$(dppm)(SnClPh$_2$)$_2$] **17** showing the atom numbering scheme. Details as in Fig. 1

The results of a single-crystal X-ray analysis of complex **17** are illustrated in Fig. 4 and selected bond distances and angles are given in Table 3. An almost octahedral environment is observed around the Fe atom, formed by three *mer*-carbonyls, two Sn atoms and one phosphorus atom of the dppm ligand. Interestingly the Fe–Sn(1) distance of 2.603(1) Å of the Sn atom *trans* to the phosphine ligand is not significantly different from the one in *cis* position: Fe–Sn(2) 2.608(1) Å. A similar observation has previously been made for the related complex *mer,cis*-[Fe(CO)$_3$(PPh$_3$)(SnClMe$_2$)$_2$].[25] It is interesting that in

Table 3 Selected bond distances (Å) and angles (°) in *mer,cis*-$[Fe(CO)_3(dppm)(SnClPh_2)_2]$ **17**

Sn(1)–Fe	2.603(1)	Fe–C(3)	1.797(9)
Sn(1)–C(11)	2.438(3)	P(1)–C(4)	1.844(8)
Sn(1)–C(29)	2.149(9)	P(1)–C(5)	1.818(8)
Sn(1)–C(35)	2.15(1)	P(1)–C(11)	1.822(8)
Sn(2)–Fe	2.608(1)	P(2)–C(4)	1.819(8)
Sn(2)–C(12)	2.511(2)	P(2)–C(17)	1.824(8)
Sn(2)–C(41)	2.152(8)	P(2)–C(23)	1.804(9)
Sn(2)–C(47)	2.153(9)	O(1)–C(1)	1.109(9)
Fe–P(1)	2.270(2)	O(2)–C(2)	1.13(1)
Fe–C(1)	1.812(9)	O(3)–C(3)	1.137(9)
Fe–C(2)	1.80(1)	Sn(2) · · · P(2)	3.140(2)
Sn(1) · · · Cl(2)	3.262(2)		
Fe–Sn(1)–Cl(1)	101.0(1)	P(1)–Fe–C(1)	86.5(3)
Fe–Sn(1)–C(29)	115.3(2)	P(1)–Fe–C(2)	96.2(3)
Fe–Sn(1)–C(35)	126.3(2)	P(1)–Fe–C(3)	99.3(3)
Cl(1)–Sn(1)–C(29)	97.7(3)	C(1)–Fe–C(2)	93.4(4)
Cl(1)–Sn(1)–C(35)	93.8(3)	C(1)–Fe–C(3)	101.0(4)
C(29)–Sn(1)–C(35)	113.2(3)	C(2)–Fe–C(3)	159.4(4)
Fe–Sn(2)–Cl(2)	95.68(7)	C(4)–P(1)–C(5)	103.6(4)
Fe–Sn(2)–C(41)	122.6(2)	C(4)–P(1)–C(11)	101.9(4)
Fe–Sn(2)–C(47)	122.5(2)	C(5)–P(1)–C(11)	102.5(4)
Cl(2)–Sn(2)–C(41)	91.9(3)	C(4)–P(2)–C(17)	103.3(4)
Cl(2)–Sn(2)–C(47)	97.9(3)	Sn(2)–Fe–C(1)	175.1(3)
C(41)–Sn(2)–C(47)	112.4(3)	Sn(2)–Fe–C(2)	84.3(3)
Sn(1)–Fe–Sn(2)	90.71(4)	Sn(2)–Fe–C(3)	80.3(2)
Sn(1)–Fe–P(1)	171.2(1)	C(4)–P(2)–C(23)	105.2(4)
Sn(1)–Fe–C(1)	84.8(3)	C(17)–P(2)–C(23)	101.7(4)
Sn(1)–Fe–C(2)	86.0(3)	P(1)–C(4)–P(2)	112.8(4)
Sn(1)–Fe–C(3)	80.8(2)	P(2)–Sn(2)–Cl(2)	169.1(8)
Sn(2)–Fe–P(1)	98.01(6)		

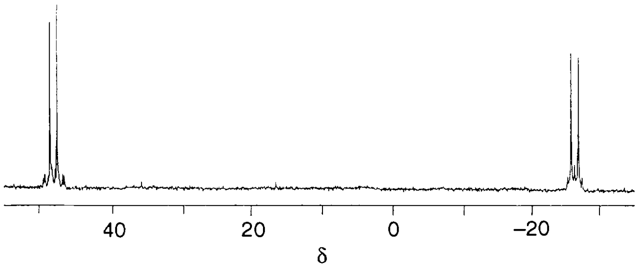

Fig. 5 The $^{31}P-\{^1H\}$ NMR spectrum of complex **17** in $CH_2Cl_2-C_6D_6$ at 298 K

complexes of type *mer*-$[Fe(CO)_3(PR_3)(SiR'_3)_2]$ a shortening of the Fe–Si bond *trans* to phosphorus is usually observed owing to the better donor ability of phosphines. Obviously, the Fe–Sn bonds are less affected by the nature of the ligand in *trans* position. The co-ordination sphere around the Sn atoms is tetrahedral, formed by two phenyl groups and a chlorine atom. The angles about Sn(1) range from 97.7(3) [for Cl(1)–Sn–C(29)] to 126.3(2)° [for Fe–Sn(1)–C(35)]. Those about Sn(2) are found in the range 97.9(3) [for Cl(2)–Sn(2)–C(47)] to 122.6(2)° [for Fe–Sn(2)–C(41)]. The P(2)–Sn(2) distance of 3.140(2) Å seems too long to represent a significant bonding interaction although the deformation of the Sn(2) co-ordination geometry towards trigonal bipyramidal would tend to support some interaction between P(2) and Sn(2).

An AX pattern is observed in the $^{31}P-\{^1H\}$ NMR spectrum of complex **17** (Fig. 5). The first doublet resonance at δ 47.5 with a $^2J(P-P)$ = 83 Hz is attributed to an iron-bound phosphorus atom, coupled to two sets of $^{117,119}Sn$ isotopes with $^2J(P-Sn)$ = 121 and 157 Hz, corresponding to the two chemically different Sn atoms. A second doublet is observed at δ −26.7, which displays a small $^1J(P-Sn)$ coupling of 85 Hz, consistent with a weak co-ordinating interaction with a Sn atom. This coupling appears too large to represent a ^4J but rather a $^1J(P-Sn)$ coupling. The discrepancy between the solid-state and solution data could either be due to a solid-state effect and/or to an exchange process arising from rapid oscillation of the dppm ligand around the observed minimum-energy position. We recently observed a similar phenomenon in related dppm-bridged iron–mercury complexes, where coupling between a dppm-phosphorus atom and ^{199}Hg was observed, however without a bonding interaction in the solid state.[26] No intramolecular interaction was observed between Cl(2) and Sn(1) [3.262(2) Å] although it is noteworthy that in *mer,cis*-$[Fe(CO)_3(PPh_3)(SnMe_2Cl)_2]$ the possibility of intramolecular $Sn(\mu-Cl)_2Sn$ bridging at low temperature was discussed.[25,27] Such an exchange process could also affect the geometry about the Sn(2) atom and influence the P(2)–Sn couplings. Complex **17** appears to be the first fully characterised metal–tin complex containing a (incipient) bridging dppm ligand.

Based on spectroscopic and structural data we suggest the following sequence for the reaction in Scheme 5: first the trimetallic complex **16** is formed by KCl elimination, which then reacts with excess of $SnCl_2Ph_2$ with formal elimination of $SiCl(OMe)_3$ (not characterised) to yield **17**. We observed an acceleration of this subsequent reaction when the solution was exposed to air: the presence of humidity could promote the rupture of the Fe–Si bonds. The silyl group on Fe may thus be regarded as a protecting group for a negative charge on the metal centre, which could under certain conditions become accessible for selective electrophilic reagents. The driving force for the observed reaction could be the higher stability of Fe–Sn compared to Fe–Si bonds.[28] Related Ru–Si for Ru–Sn exchange reactions have previously been observed by Knox and Stone.[29a] Four-membered cyclic intermediates could be involved in these transformations, as proposed in exchange reactions of $HgBr_2$ with $[Fe(C_5H_5)(CO)_2(SnR_3)]$ to yield Fe–Hg bonds with formal $SnBrR_3$ elimination.[29b]

Attempts to use complex **17** as a precursor in reactions with metalates like $[Mn(CO)_5]^-$ in order to form chain complexes or clusters were unsuccessful and reaction with $TlPF_6$ in CH_2Cl_2 did not allow isolation of the anticipated cationic species.

Phosphino-pyridine Bridged Fe–M (M = Zn, Ga *or* In) *Chain Complexes.*—2-(Diphenylphosphino)pyridine was reported in 1944[30] and used by Balch and co-workers[31] to assemble different metal centres. We recently prepared $(Ph_2P)C_5H_4N$-bridged iron–cadmium complexes starting from **2d**.[3h] We were interested to extend our comparative study of the use of dppm and $(Ph_2P)C_5H_4N$ as stabilising ligands in heterobimetallic complexes to systems containing Zn, Cd, Hg, Ga or In. In addition, the oxophilic atom seemed to be a promising candidate for the formation of a Fe–Si–O→Zn interaction and C–Si–O–Zn four-membered rings have recently been reported.[32]

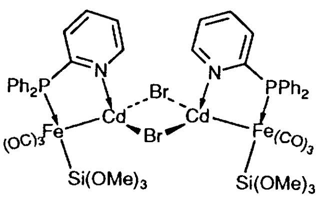

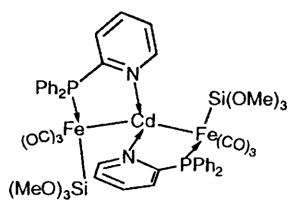

Reaction of complex **2d** with an excess of $ZnCl_2$ or ZnI_2 yielded the new complexes **18** and **19** in high yields as thf solvates. In contrast to their dppm-bridged analogues these new compounds showed no tendency to decompose in solution.[3f] In order to gain more information about the extent of Fe–Si–O→Zn interactions, we carried out a variable-temperature NMR investigation on a thf-free sample of *mer*-$[\{[(MeO)_3Si](OC)_3Fe[\mu-(Ph_2P)C_5H_4N]Zn(\mu-Cl)\}_2]$ **18**. As in all other $(Ph_2P)C_5H_4N$-bridged complexes described in this paper, the proton in the 6 position of the pyridine ring gives rise to a

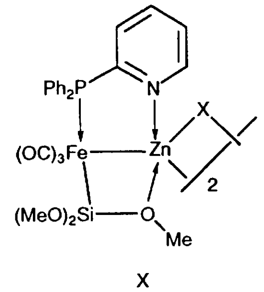

X
18 Cl
19 I

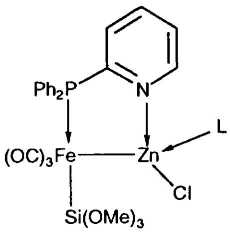

L
20 4 Me-py
21 Bu^{t}NC

doublet at *ca.* δ 9, whereas this resonance appears at higher field when the pyridine ring is not co-ordinated (as in **1d** where δ 8.25).[33] In $CDCl_3$ the ^1H NMR signal for the methoxy protons appears as a broad singlet at δ 3.68, which sharpens slightly when raising the temperature to 313 K. When cooling a CD_2Cl_2 solution this signal gradually broadens. At 195 K the signal begins to split finally to yield at 185 K two distinct peaks in an approximate 1 : 2 ratio at δ 3.60 and 3.52. We attribute this to the presence of non-equivalent methoxy groups as a result of their exchange being now sufficiently slowed down.

Our formulation of a dimeric structure for **18** and **19** is based on the instantaneous bridge splitting with 2 equivalents of 4Me-py, which gives $[\{(MeO)_3Si\}(OC)_3Fe\{\mu\text{-}(Ph_2P)C_5H_4N\}ZnCl(4Me\text{-}py)]$ **20** in quantitative yield. Owing to the further donor ligand on the zinc centre the IR carbonyl stretches are shifted *ca.* 4 cm^{-1} to lower wavenumbers compared to **19**. The chloride bridges of **19** can also be cleaved by Bu^{t}NC to yield the isocyanide complex *mer*-$[\{(MeO)_3Si\}(OC)_3Fe\{\mu\text{-}(Ph_2P)C_5H_4N\}ZnCl(Bu^tNC)]$ **21**. An equilibrium between free Bu^{t}NC [ν(NC) 2140 cm^{-1}] and the adduct [ν(NC) 2221 cm^{-1}] is observed in CH_2Cl_2 solution, whereas only one ν(NC) band at 2219 cm^{-1} is observed in the solid state (KBr). The ^1H NMR spectrum remains almost unchanged in the temperature range 298–223 K, showing sharp singlets at δ 1.43 and 3.68 for the Bu^t and the methoxy groups, respectively.

The acidic hydride ligand of complex **1d** reacts smoothly with $ZnEt_2$ to give the alkyl complex *mer*-$[\{(MeO)_3Si\}(OC)_3Fe\{\mu\text{-}(Ph_2P)C_5H_4N\}ZnEt]$ **22** which is less stable than the halogen-containing complexes described before. The ^1H NMR spectrum in C_6D_6 of the crude isolated product shows, besides traces of another compound, a well resolved quartet for the methylene group at δ 1.06, a triplet for the methyl group at δ 1.77 and a sharp singlet at δ 3.97 for the methoxy protons. A quartet at δ 0.07 and a triplet resonance at δ 1.10 has been reported for $ZnEt_2$ in C_6D_6.[34] Despite this simple ^1H NMR spectrum two close resonances of equal intensity are observed at δ 87.7 and 87.3 in the $^{31}P\text{-}\{^1H\}$ NMR spectrum.

When the ferrate **2d** was treated with an excess of $InCl_3$ or $GaCl_3$ the new bimetallic complexes **23** and **24** were formed in high yields and were characterised by spectroscopic and analytical methods. Both complexes form stable and almost colourless microcrystalline powders and exhibit similar absorption patterns in their IR spectra, indicating a meridional arrangement of the carbonyl groups. The absorptions for **23** are observed in thf at 2036, 1976 and 1967 cm^{-1}. The FIR absorptions for **23** at 347 cm^{-1} and for **24** at 319 and 315 cm^{-1} are typical for the ν(M–Cl) stretches of terminal chlorine atoms on gallium and indium[9] and are comparable to those found for complexes **10** and **11**. Dimeric structures can therefore be ruled out for those complexes. In the ^1H NMR spectrum a singlet resonance was found for the $Si(OMe)_3$ protons and no splitting or broadening, was observed on decreasing the temperature, ruling out a significant Fe–Si–O→M interaction. The $^{31}P\text{-}\{^1H\}$ NMR spectrum contains a singlet resonance at δ 82.9 for **23** and δ 80.6 for **24**.

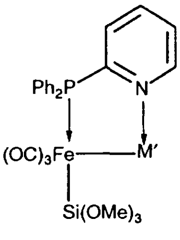

M′
22 ZnEt
23 $GaCl_2$
24 $InCl_2$

Synthesis of a $(Ph_2P)C_5H_4N$ *Bridged Trimetallic* Fe–Zn–Fe *Chain Complex.*—Unsupported Fe–Zn–Fe arrays are already known[35a] and even structurally characterised.[2,35b,c] It appeared interesting to prepare a $(Ph_2P)C_5H_4N$-bridged Fe–Zn–Fe chain and compare it with the structurally characterised Fe–Cd–Fe chain complex $[Cd\{Fe(CO)_3[Si(OMe)_3][\mu\text{-}(Ph_2P)C_5H_4N]\}_2]$.[3h]

When $ZnCl_2$ was added to a two-fold excess of complex **1d** in CH_2Cl_2 a clean IR spectrum with three vibrations at 1982m, 1925s and 1897 (sh) cm^{-1} was obtained, which was assigned to the chain complex $[Zn\{Fe(CO)_3[Si(OMe)_3][\mu\text{-}(Ph_2P)C_5H_4N\}_2]$ **25**. When removing the CH_2Cl_2 and redissolving the residue in thf, strong vibrations at 1845 and 1823 (sh) cm^{-1} were found which are very similar (and were assigned) to the anion $[Fe(CO)_3\{Si(OMe)_3\}\{(Ph_2P)C_5H_4N\}]^-$ [1920w, 1844vs and 1821s (sh) cm^{-1}].[3h] In addition, three ν(CO) vibrations at 1987, 1925 and 1904 cm^{-1} are due to the meridional carbonyls of the Fe–Zn cationic moiety. Unfortunately, this complex decomposed in an attempt to grow crystals. Based on these findings we propose the formation of a solvent-separated ion pair of the type *mer*-$[\{(MeO)_3Si\}(OC)_3Fe\{\mu\text{-}(Ph_2P)C_5H_4N\}Zn][Fe(CO)_3\{Si(OMe)_3\}\{(Ph_2P)C_5H_4N\}]$ in thf, a known feature for M–Zn–M or M–Cd–M (M = transitional metal) complexes.[36]

Synthesis of $(Ph_2P)C_5H_4N$ *Bridged Heterotrimetallic Chain Complexes.*—Since pyridine has a higher affinity than phosphines towards metals such as Zn and Cd, $(Ph_2P)C_5H_4N$ should stabilise corresponding metal–metal bonded complexes better than dppm. Thus, complexes **26–28** were synthesised and isolated in good yields when a stoichiometric amount of the metalate $Na[M(C_5H_5)(CO)_3]$ (M = Mo or W) was added to **18** or $[\{[(MeO)_3Si](OC)_3Fe[\mu\text{-}(Ph_2P)C_5H_4N]Cd(\mu\text{-}Br)\}_2]$, respectively.

Pure, colourless complex **26** was obtained by precipitation from a cold solution since it decomposes on standing with formation of among other complexes $[W_2(C_5H_5)_2(CO)_6]$. Its IR spectrum in the ν(CO) region consists of a set of three vibrations at 1990, 1927 and 1905 cm^{-1} for the iron moiety and three vibrations at 1954, 1864 and 1837 cm^{-1} for the tungsten moiety. In the proton NMR spectrum the methoxy groups appear as a sharp singlet at δ 3.88 and the C_5H_5 protons as a

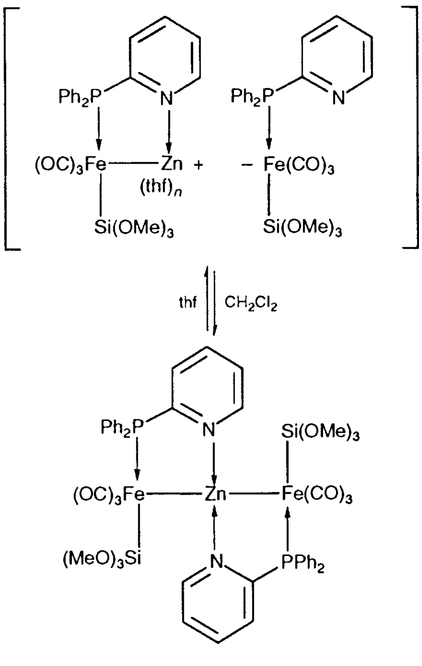

25

Scheme 6

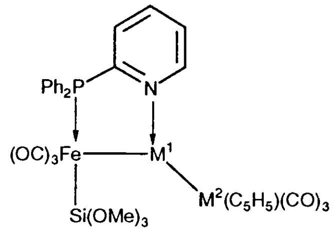

	M^1	M^2
26	Zn	W
27	Cd	Mo
28	Cd	W
29	Hg	W
30	InCl	W

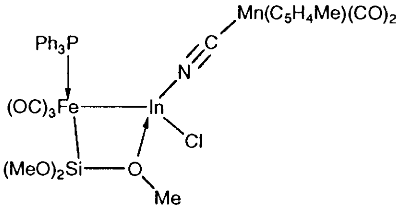

31

singlet at δ 5.32. The Fe–Cd–Mo complex **27** is labile and could only be identified by IR spectroscopy, whereas the analogous Fe–Cd–W chain complex **28** was isolated as a more stable, colourless powder. The pattern of its ν(CO) stretches is almost identical with that of **26**. The ^{31}P-$\{^1$H$\}$ NMR spectrum displays a very sharp singlet at δ 82.7, which is flanked by satellites due to ^{2+3}J(P–^{111,113}Cd) 63 Hz and to ^{3+4}J(P–^{183}W) 12 Hz (natural abundance of ^{183}W = 14.2%).

The more labile derivative **29** was obtained by reaction of **2d** with [W(C$_5$H$_5$)(CO)$_3$(HgCl)][1a] in thf and was characterised by spectroscopic and analytical methods. Two sets of satellites due to ^{2+3}J(P–^{199}Hg) 170 Hz and ^{3+4}J(P–^{183}W) 28 Hz are observed. The pattern of the ν(CO) stretches within the series **26**, **28**, **29** remains almost identical, a slight shift to higher wavenumbers being observed due to the decreasing polarity of the metal–metal bonds on going from Zn to Hg.

The reaction of complex **24** with 1 equivalent of Na[W(C$_5$H$_5$)(CO)$_3$] yielded a stable, yellow powder of *mer*-[{(MeO)$_3$Si}(OC)$_3$Fe{μ-(Ph$_2$P)C$_5$H$_4$N}InCl{W(C$_5$H$_5$)(CO)$_3$}] **30** which was characterised by usual analytical and spectroscopic methods. Two sets of absorptions were observed in the IR spectrum for the *mer*-Fe(CO)$_3$ and the (C$_5$H$_5$)W(CO)$_3$ fragments (Table 4). Compared to **24** the values of the absorptions of the iron-bound carbonyls of **30** are decreased by 15 cm^{-1}, consistent with an increased electron density in the trimetallic system. The FIR spectrum shows a ν(In–Cl) absorption for a terminal chlorine atom at 261 cm^{-1}.[9] In the ^{1}H NMR spectrum singlet resonances are found for the Si(OMe)$_3$ group at δ 3.73 and the C$_5$H$_5$ group at δ 5.54. A singlet resonance is observed at δ 80.6 in the ^{31}P-$\{^1$H$\}$ NMR spectrum with ^{3+4}J(P–^{183}W) of 10 Hz.

Heterometallic Complexes with a (C$_5$H$_4$Me)Mn(CO)$_2$(CN)] *Fragment.*—The cyanometalate [Mn(C$_5$H$_4$Me)(CO)$_2$(CN)]$^-$ has been used previously as a nucleophile (through its nitrogen atom) in reactions with Group 14 and 15 electrophiles, affording products of the type M–CN–E (E = P or As).[37] Only a few examples of reactions with transition-metal halides to yield cyano-bridged heterometallic complexes have been reported.[8]

Addition of solid Na[Mn(C$_5$H$_4$Me)(CO)$_2$(CN)] to a toluene solution of complex **3** gave the new complex *mer*-[{(MeO)$_3$Si}(Ph$_3$P)(OC)$_3$FeInCl{(NC)Mn(C$_5$H$_4$Me)(CO)$_2$}] **31** in good yields as orange crystals which were characterised by analytical and spectroscopic methods. The IR spectrum of a toluene solution of it shows three characteristic absorptions of the *mer*-Fe(CO)$_3$ carbonyls (Table 5). Two strong absorptions are observed for the manganese carbonyls at 1923 and 1872 cm^{-1}. The ν(CN) absorption was found at 2047 cm^{-1}. All resonances in the ^{1}H NMR spectrum were broad and not resolved at various temperatures. The ^{31}P-$\{^1$H$\}$ NMR spectrum displayed at 298 K a very broad signal at δ 56 which sharpened upon raising the temperature to 323 K to yield a singlet at δ 54.5.

In order better to understand the NMR features of complex **31** and to obtain comparative data we prepared [(OC)$_2$(C$_5$H$_4$Me)Mn(CN)InCl$_2$] **32** by reaction of Na[Mn(C$_5$H$_4$Me)(CO)$_2$(CN)] with InCl$_3$ in toluene. Bright yellow and air-sensitive **32** was formed in almost quantitative yields and was characterised by IR and ^{1}H NMR spectroscopy. Its ^{1}H NMR spectrum showed two broad resonances at δ 1.5 and 4.3, corresponding to the three methyl and four C$_5$H$_4$ protons, respectively.

Related (Ph$_2$P)C$_5$H$_4$N-bridged complexes were obtained in quantitative spectroscopic yields when **18** or *mer*-[{[(MeO)$_3$Si](OC)$_3$Fe{μ-(Ph$_2$P)C$_5$H$_4$N}Cd(μ-Br)}$_2$][3h] were treated with Na[Mn(C$_5$H$_4$Me)(CO)$_2$(CN)] in thf. Whereas the Fe–Cd–NC–Mn complex **34** is stable, the lability of **33** did not allow a satisfactory elemental analysis. As already described in the case of **31** and **32**, the ^{1}H NMR spectra of **33** and **34** showed very broad resonances at high and low temperatures, precluding an unequivocal interpretation. The resolution problems may also be due to the formation of paramagnetic impurities. The ^{31}P-$\{^1$H$\}$ NMR spectrum of **34** showed a singlet resonance at δ 85.4 flanked by cadmium satellites with ^{2+3}J(P–^{111,113}Cd) 87 Hz. These NMR features could be due to the presence of several conformers and a low rotational barrier along the M′–CN–M axis. Furthermore a possible Fe–Si–O→M′ interaction may complicate the situation. Especially in the case of **33** and **34** the tendency of Zn and Cd to attain a tetrahedral environment makes this bonding mode likely.

Table 4 Selected IR data (cm^{-1}) (thf solution)

Complex	ν(CO), *mer*-Fe(CO)$_3$	ν(CO), (C$_5$H$_5$) or (C$_5$H$_4$Me)M(CO)$_3$
12	2011m, 1950 (sh), 1944s	1980vs, 1917s, 1861s
13	2010m, 1950 (sh), 1943s	1979vs, 1910s, 1857s
14	1983m, 1919s, 1899vs	1955vs, 1871s, 1836vs
26	1990m, 1927s, 1905vs	1954s, 1864m, 1837m
27	1988m, 1922 (sh), 1907vs	1955vs, 1874s, 1846s
28	1988m, 1928m, 1904vs	1955vs, 1868s, 1840s
29	2004m, 1964,[a] 1929s	1964vs,[a] 1889s, 1872s
30[b]	2015w, 1957m, 1944s	1981vs, 1904m, 1877m

[a] Partial overlap with an absorption of the other fragment. [b] In CH$_2$Cl$_2$ solution.

Table 5 Selected IR data (cm^{-1}) (toluene solution)

Complex	ν(CO) *mer*-Fe(CO)$_3$	ν(CO)(C$_5$H$_4$Me)Mn(CO)$_2$	ν(CN)
31	2027m, 1972vs, 1958 (sh)	1923vs, 1872s	2047m
32	--	1922s, 1870s	2041m
33	1992m, 1920vs, 1910 (sh)	1910,* 1857s	2068m
34	1991m, 1919vs, 1911 (sh)	1910,* 1858s	2060m

* Partial overlap with an absorption of the other fragment.

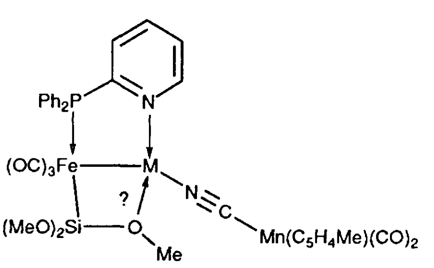

	M
33	Zn
34	Cd

Conclusion

We have shown that metalates with pendant donor ligands are versatile precursors for the systematic synthesis of polymetallic complexes containing main group–transition metal combinations. Ligands like dppm or (Ph$_2$P)C$_5$H$_4$N stabilise for instance the Fe–M bond (M = Ga or Zn) in complexes **10**, **18** and **24**, whereas in the absence of such bridging ligands, spontaneous dissociation of the Fe–M bond occurs under formation of hydrides of type **1**. Another interesting aspect of this stabilising effect is the rational access to rare heterotrimetallic complexes such as **13**, **14** and **26**–**34**. Although heterotrimetallic chains of the type M^1–M^2–M^3 often undergo spontaneous rearrangement reactions to form symmetric products, most of our new complexes were stable and did not show such a reactivity. We consider the presence of the bridging ligand an important condition for this stabilising effect.

Complex **17** contains a novel dppm-bridged Fe–Sn array, demonstrating again the high synthetic versatility of precursors of type **2**. The cleavage of a metal-silicon bond is the crucial step in the formation of **17**. Easy element–silicon bond cleavage is widely used in the synthesis of large clusters[39] and therefore silyl-substituted polynuclear complexes could become interesting precursors for the stepwise increase in nuclearity in cluster synthesis.

Another interesting aspect resides in further examples of the rare Fe–Si–O$\rightarrow$M interaction found in **6**–**9**, **18** and **19**. The previously observed lability of this interaction makes such kind of complexes interesting for reactivity studies. They may also represent possible models for catalytic systems involving silica surfaces.[3m] Low-temperature NMR studies allowed estimates of $\Delta G^\ddagger$ for the O$\rightarrow$M bond (42–54 kJ mol^{-1}). This energy is considerably lower than the values found in Pt/Pd/Rh-containing complexes (60–65 kJ mol^{-1}) which is consistent with the shorter O–M distances found in the latter cases. However, oxygen is usually considered as a hard donor ligand and theory predicts a stronger bonding interaction with hard acids (like Group 12 and 13 elements) than with soft acids (such as group 8–10 transition metals). At the present stage we cannot give a conclusive interpretation of this finding, and further investigations are needed.

Experimental

Syntheses.—All experiments were carried out using Schlenk-tube techniques, under an atmosphere of oxygen-free nitrogen. Elemental C, H and N analyses were performed by the Service Central de Microanalyses du CNRS. Infrared spectra were obtained using Perkin Elmer 398 or Bruker IFS 66/113 (FTIR) spectrometers, and NMR spectra on a Bruker SY200 instrument with proton chemical shifts measured relative to tetramethylsilane and phosphorus chemical shifts relative to phosphoric acid (external reference) with downfield chemical shifts reported as positive. The reactions were generally monitored by IR spectroscopy in the ν(CO) region. Unless otherwise specified, the pure complexes are air-stable in the solid state for prolonged periods. Selected IR data are presented in Tables 4 and 5.

mer-[{[(MeO)$_3$Si](Ph$_3$P)(OC)$_3$FeIn(μ-Cl)Cl}$_2$] **3**.—The compound K[Fe(CO)$_3$(PPh$_3$){Si(OMe)$_3$}] (0.562 g, 1.0 mmol) in thf (25 cm^3) was added at 0 °C to a solution of InCl$_3$ (0.243 g, 1.1 mmol) in thf (5 cm^3). The yellow reaction mixture was stirred for 0.5 h at room temperature and then filtered to remove KCl. After evaporation of the solvent to dryness the residue was extracted with CH$_2$Cl$_2$ (5 cm^3) and filtered again. Addition of cold hexane induced the precipitation of a white powder, which was dried *in vacuo*. Keeping the mother-liquor in the cold for 2 d afforded a further crop of colourless microcrystals (0.61 g, 83%) (Found: C, 39.75; H, 3.25. Calc. for C$_{48}$H$_{48}$Cl$_4$Fe$_2$In$_2$O$_{12}$P$_2$Si$_2$: C, 40.65; H, 3.40%). IR: ν(CO) (CH$_2$Cl$_2$) 2034m, 1979 (sh) and 1969vs; (thf) 2025m, 1973 (sh) and 1955vs; (KBr) 2024ms and 1963vs cm^{-1}. FIR (polyethylene): ν(InCl$_{\text{terminal}}$) 320s; ν(InCl$_{\text{bridge}}$) 254m, 250m and 200w cm^{-1}. NMR: ^{1}H (200 MHz, CDCl$_3$), δ 3.75 (s, 9 H, OCH$_3$) and 7.26–7.62 (m, 15 H, C$_6$H$_5$); ^{31}P-{^{1}H} (81.02 MHz, δ(C$_6$D$_6$–CH$_2$Cl$_2$) 53.5 [s, P(Fe)], (C$_6$D$_6$–thf) 56.3 [s, P(Fe)].

mer-[{[(MeO)$_3$Si](Ph$_3$P)(OC)$_3$FeIn(μ-Br)Br}$_2$] **4**.—*Method* 1. Solid KBr (0.041 g, 0.35 mmol) was added to a solution of complex **3** (0.100 g, 0.071 mmol) in CH$_2$Cl$_2$ (5 cm^3). The yellow reaction mixture was stirred for several hours at room temperature and then filtered to remove excess of KBr. An equivalent volume of hexane was added and the solution was evaporated under reduced pressure until the beginning of precipitation. The solution was left for 24 h at −30 °C and pale yellow crystals formed (0.102 g, 90%).

Method 2. A procedure analogous to that described for the synthesis of complex **3** using InBr$_3$ also led to **4** (Found: C, 36.25; H, 3.00. Calc. for C$_{48}$H$_{48}$Br$_4$Fe$_2$In$_2$O$_{12}$P$_2$Si$_2$: C, 36.10; H, 3.05%). IR: ν(CO) (CH$_2$Cl$_2$) 2033m, 1978 (sh), 1968vs; (KBr) 2034s, 1992m, 1961vs and 1930vw cm^{-1}. FIR (polyethylene): ν(InBr) 228s (br) cm^{-1}. NMR: ^{1}H (200 MHz, CDCl$_3$), δ 3.75 (s, 9 H, OCH$_3$) and 7.50–7.58 (m, 15 H, C$_6$H$_5$); ^{31}P-{^{1}H} (81.02 MHz, C$_6$D$_6$–CH$_2$Cl$_2$), δ 53.5 [s, P(Fe)].

mer-[{[(MeO)$_3$Si](Ph$_3$P)(OC)$_3$FeIn(μ-I)I}$_2$] **5**.—This synthesis was analogous to that of complex **4** (method 1) with KI (0.058 g, 0.35 mmol) and **3** (0.100 g, 0.071 mmol) and afforded a yellow, microcrystalline product. Yield (0.11 g, 90%) (Found: C, 32.90; H, 2.80. Calc. for $C_{48}H_{48}Fe_2I_4In_2O_{12}P_2Si_2$: C, 32.30; H, 2.70%). IR: ν(CO) (CH_2Cl_2) 2031m, 1976 (sh) and 1966vs cm^{-1}. FIR (polyethylene): 316w, 299vw, 261vw, 226w, 209m and 189s cm^{-1}. NMR: ^{1}H (200 MHz, $CDCl_3$), δ 3.73 (s, 9 H, OCH_3) and 7.26–7.56 (m, 15 H, C_6H_5); ^{31}P-{^{1}H} (81.02 MHz, C_6D_6–CH_2Cl_2), δ 53.8 [s, P(Fe)].

mer-$[(Ph_3P)(OC)_3Fe\{\mu\text{-}Si(OMe)_2(OMe)\}InCl_2(OPPh_3)]$ **6**.—Triphenylphosphine oxide (0.085 g, 0.323 mmol) was added to a solution of complex **3** (0.325 g, 0.162 mmol) in CH_2Cl_2 (20 cm^3). The clear solution was stirred for 5 min. Addition of hexane precipitated yellowish microcrystals, which were dried *in vacuo* (0.30 g, 95%). Slow diffusion of hexane into a chlorobenzene solution at 5 °C afforded bright yellow crystals which were suitable for X-ray analysis (Found: C, 47.05; H, 3.90. Calc. for $C_{42}H_{39}Cl_2FeInO_7P_2Si\cdot1.5CH_2Cl_2$: C, 46.85; H, 3.80%). IR: ν(CO) (CH_2Cl_2): 2024m, 1969s, 1953vs; (KBr) 2018s, 1969s and 1944vs cm^{-1}. FIR (polyethylene): ν(InCl) 302s and 296s cm^{-1}. NMR: ^{1}H (200 MHz, $CDCl_3$) (298 K), δ 3.62 (s, 9 H, OCH_3) and 7.26–7.55 (m, 30 H, C_6H_5); (223 K) 3.36 (s, 3 H, OCH_3), 3.64 (s, 6 H, OCH_3) and 7.15–7.77 (m, 30 H, C_6H_5); ^{31}P-{^{1}H} (81.02 MHz, CH_2Cl_2–$CDCl_3$), δ 56.1 [s, P(Fe)] and 35.7 (br, $OPPh_3$).

mer-$[(Ph_3P)(OC)_3Fe\{\mu\text{-}Si(OMe)_2(OMe)\}InCl_2(4Me\text{-}py)]$ **7**.—To a solution of complex **3** (0.050 g, 0.035 mmol) in CH_2Cl_2 (6 cm^3) was added *via* microsyringe 4Me-py (7 μl, 0.07 mmol). The clear solution was stirred for 5 min, then the solvent was removed and the residue dried *in vacuo* for several hours (0.053 g, 95%) (Found: C, 45.3; H, 4.9; N, 1.3. Calc. for $C_{30}H_{31}Cl_2FeInNO_6PSi$: C, 44.90; H, 3.90; N, 1.75%). IR: ν(CO) (CH_2Cl_2) 2024m, 1968 (sh), 1952vs; (KBr) 2026s, 1979s and 1950vs cm^{-1}. FIR (polyethylene): ν(InCl) 303s (br) cm^{-1}. NMR: ^{1}H (200 MHz, $CDCl_3$), δ 2.25 (s, 3 H, CH_3), 3.49 (s, 9 H, OCH_3) and 7.21–7.54 (m, 19 H, C_6H_5, C_5H_4N); ^{31}P-{^{1}H} (81.02 MHz, CH_2Cl_2–C_6D_6), δ 54.3 [s, P(Fe)].

mer-$[InCl\{Fe(CO)_3(PPh_3)[\mu\text{-}Si(OMe)_2(OMe)]\}_2]$ **8**.—*Method* 1. The complex $K[Fe(CO)_3(PPh_3)\{Si(OMe)_3\}]$ (0.563 g, 1 mmol) in thf (25 cm^3) was slowly added at 0 °C to a solution of **3** (0.709 g, 0.5 mmol) in thf (10 cm^3). The yellow reaction mixture was stirred for 1 h at room temperature and then filtered to remove KCl. After evaporation of the solvent to dryness the residue was dissolved in CH_2Cl_2 (5 cm^3). Slow diffusion of hexane into the solution afforded yellow crystals (0.96 g, 80%).

Method 2. The complex $K[Fe(CO)_3(PPh_3)\{Si(OMe)_3\}]$ (0.563 g, 1 mmol) in thf (25 cm^3) was slowly added at 0 °C to a solution of $InCl_3$ (0.111 g, 0.5 mmol). The work-up and yield were similar to those in Method 1 (Found: C, 45.60; H, 4.00. Calc. for $C_{48}H_{49}ClFe_2InO_{12}P_2Si_2\cdot CH_2Cl_2$: C, 45.90; H, 4.00%). IR (KBr): ν(CO) 2005s, 1974vs, 1966s, 1952vs and 1936vs cm^{-1}. FIR (polyethylene): ν(InCl) 286s cm^{-1}. NMR: ^{1}H (200 MHz, CD_2Cl_2) (298 K), δ 3.47 (s, 18 H, OCH_3) and 7.40–7.60 (m, 30 H, C_6H_5); (183 K) 2.89, 3.56 and 3.65 (s, 6 H, OMe); ^{31}P-{^{1}H} (81.02 MHz, C_6D_6–CH_2Cl_2), δ 57.4 [s, P(Fe)].

mer-$[InCl(O{=}PPh_3)\{Fe(CO)_3(PPh_3)[Si(OMe)_3]\}_2]$ **9**.—Solid triphenylphosphine oxide (0.023 g, 0.083 mmol) was added to a solution of complex **8** (0.100 g, 0.083 mmol) in CH_2Cl_2 (20 cm^3). The clear solution was stirred for 0.5 h. Addition of hexane and cooling to −30 °C yielded colourless crystals, which were dried *in vacuo* (0.117 g, 95%). IR (KBr): ν(CO) 2028m, 1981m and 1951vs cm^{-1}. FIR (polyethylene): ν(InCl) 290 (br) cm^{-1}. NMR: ^{1}H (200 MHz, CD_2Cl_2 (298 K), δ 3.57 (s, 18 H, OCH_3) and 7.36–7.59 (m, 45 H, C_6H_5); (203 K) 3.25 (s, 6 H, OCH_3), 3.56 (s, 12 H, OCH_3) and 7.02–7.77 (m, 45 H, C_6H_5); ^{31}P-{^{1}H} (81.02 MHz, CH_2Cl_2–C_6D_6), δ 57.4 [s, P(Fe)] and 28.1 (br s, $OPPh_3$).

mer-$[\{(MeO)_3Si\}(OC)_3Fe(\mu\text{-}dppm)GaCl_2]$ **10**.—A solution of $K[Fe(CO)_3\{Si(OMe)_3\}(dppm\text{-}P)]$ (0.685 g, 1 mmol) in thf (5 cm^3) was added at 0 °C to a solution of $GaCl_3$ (0.194 g, 1.1 mmol) in thf (5 cm^3). The yellow reaction mixture was stirred for 0.5 h at room temperature and then filtered to remove KCl. After evaporation of the solvent to dryness the residue was extracted with CH_2Cl_2 (5 cm^3) and filtered again. Addition of cold diethyl ether induced the precipitation of a yellowish powder, which was dried *in vacuo*. Keeping the mother-liquor in the cold for 2 d afforded a further crop of yellowish microcrystals (0.63 g, 80%) (Found: C, 47.40; H, 4.15. Calc. for $C_{31}H_{31}Cl_2GaFeO_6P_2Si$: C, 47.35; H, 4.00%). IR (thf): ν(CO) 2030m, 1972 (sh) and 1959s cm^{-1}. FIR (polyethylene): 370s (br), 340s (br) and 150m (br). NMR: ^{1}H (200 MHz, $CDCl_3$), δ 3.26 [t, 2 H, CH_2, ^2J(P–H) = 10.3], 3.75 (s, 9 H, OCH_3) and 7.18–7.61 (m, 20 H, C_6H_5); ^{31}P-{^{1}H} (81.02 MHz, C_6D_6–thf), δ 62.5 [d, P(Fe), ^{2+3}J(P–P) = 125 Hz] and −15.7 [d, P(Ga)].

mer-$[\{(MeO)_3Si\}(OC)_3Fe(\mu\text{-}dppm)InCl_2]$ **11**.—A solution of $K[Fe(CO)_3\{Si(OMe)_3\}(dppm\text{-}P)]$ (0.685 g, 1.0 mmol) in thf (5 cm^3) was added at 0 °C to a solution of $InCl_3$ (0.243 g, 1.1 mmol) in thf (5 cm^3). The reaction mixture was stirred for 2 h, then the clear solution was filtered and the solvent was removed. The residue was extracted with CH_2Cl_2 (10 cm^3), filtered again and the solution was concentrated to *ca.* 5 cm^3 under reduced pressure. Addition of hexane afforded colourless microcrystals, which were dried *in vacuo* (0.75 g, 90%) (Found: C, 42.35; H, 3.80. Calc. for $C_{31}H_{31}Cl_2FeInO_6P_2Si$: C, 44.80; H, 3.75%). IR: ν(CO) (thf) 2020s, 1963 (sh), 1950vs; (KBr) 2018m, 1965s and 1943vs cm^{-1}. FIR (polyethylene): ν(InCl) 314s and 303s cm^{-1}. NMR: ^{1}H(200 MHz, $CDCl_3$), δ 3.12 [t, 2 H, CH_2, ^2J(P–H) = 10.1], 3.77 (s, 9 H, OCH_3) and 7.18–7.59 (m, 20 H, C_6H_5); ^{31}P-{^{1}H} (81.02 MHz, thf–C_6D_6), δ 60.7 [d, P(Fe), ^{2+3}J(P–P) = 103 Hz] and −17.5 [br d, P(In)].

mer-$[\{(MeO)_3Si\}(OC)_3Fe(\mu\text{-}dppm)InCl\{Mo(C_5H_4Me)(CO)_3\}]$ **12**.—Solid $Na[Mo(C_5H_4Me)(CO)_3]\cdot$dme (dme = 1,2-dimethoxyethane) (0.480 g, 1.1 mmol) was added at 0 °C to a solution of complex **11** (0.831 g, 1 mmol) in thf (20 cm^3). The reaction mixture was stirred for 2 h. The resulting solution was filtered to remove NaCl and the solvent was concentrated to 3 cm^3. Slow diffusion of hexane into the thf solution afforded yellow crystals, which were dried *in vacuo* (0.79 g, 70%). Slow diffusion of hexane into a chlorobenzene solution at 5 °C afforded bright yellow crystals which were suitable for X-ray analysis (Found: C, 45.35; H, 3.60. Calc. for $C_{40}H_{38}ClFeInMoO_9P_2Si$: C, 45.55; H, 3.65%). FIR (polyethylene): 261m [ν(In–Cl)] and 165m cm^{-1}. NMR: ^{1}H (200 MHz) ($CDCl_3$), δ 2.04 (s, C H, CH_3), 3.52 (m, 2 H, CH_2), 3.75 (s, 9 H, OCH_3), 5.4 (m, 4 H, C_5H_4) and 6.96–7.69 (m, 20 H, C_6H_5); (C_6D_6), δ 1.37 (s, 3 H, CH_3), 3.31 (m, 2 H, CH_2), 3.82 (s, 9 H, OCH_3), 5.13, 5.29 (m, 4 H, C_5H_4) and 6.72–7.71 (m, 20 H, C_6H_5); ^{31}P-{^{1}H} (81.02 MHz, thf–C_6D_6), δ 59.7 [d, P(Fe), ^{2+3}J(P–P) = 122 Hz] and −17.6 [br d, P(In)].

mer-$[\{(MeO)_3Si\}(OC)_3Fe(\mu\text{-}dppm)InCl\{W(C_5H_5)(CO)_3\}]$ **13**.—The synthesis was similar to that described for complex **12**. The salt $Na[W(C_5H_5)(CO)_3]\cdot$dme (0.650 g, 1.1 mmol) and **11** (0.831 g, 1.0 mmol) gave yellow crystals (0.68 g, 60%) (Found: C, 43.45; H, 3.90. Calc. for $C_{39}H_{36}ClFeInO_9P_2SiW\cdot$thf: C, 43.00; H, 3.70%). NMR: ^{1}H (200 MHz, $CDCl_3$), δ 3.52 (m, 2 H, CH_2), 3.75 (s, 9 H, OCH_3), 5.52 (s, 5 H, C_5H_5) and 6.96–7.69 (m, 20 H, C_6H_5); ^{31}P-{^{1}H} (81.02 MHz, thf–C_6D_6), δ 60.0 [d, P(Fe), ^{2+3}J(P–P) = 120 Hz] and −18.6 [br d, P(In)].

mer-$[\{(MeO)_3Si\}(OC)_3Fe(\mu\text{-}dppm)Cd\{Mo(C_5H_4Me)(CO)_3\}]$ **14**.—Solid $Na[Mo(C_5H_4Me)(CO)_3]\cdot$dme (0.480 g, 1.1 mmol) was added to a solution of *mer*-$[\{[(MeO)_3Si](OC)_3Fe(\mu\text{-}dppm)Cd(\mu\text{-}Cl)\}_2]$ (0.793 g, 0.5 mmol) in thf (10 cm^3). The reaction mixture was stirred for 0.5 h. The resulting solution was filtered to remove NaCl and the solvent was concentrated to 3 cm^3. Similar spectroscopic data were obtained when a solution of K[Fe(CO)$_3${Si(OMe)$_3$}(dppm-*P*)] was treated with [BrCdMo(C$_5$H$_4$Me)(CO)$_3$]. The resulting solution was used for IR and ^{31}P-{^{1}H} NMR spectroscopy. Complex **14** could not be isolated pure. NMR: ^{31}P-{^{1}H} (81.02 MHz, thf–C$_6$D$_6$), δ 64.3 [d, P(Fe), ^{2+3}J(P–P) = 113, ^{3+2}J(P–^{111,113}Cd) = 61] and −15.4 [d, P(Cd), ^1J(P–^{111,113}Cd) = 398 Hz].

mer-[{[(MeO)$_3$Si](OC)$_3$Fe(μ-dppb)In(μ-Cl)Cl}$_2$] **15**.—The complex K[Fe(CO)$_3${Si(OMe)$_3$}(dppb-*P*)] (0.726 g, 1.0 mmol) in thf (20 cm^3) was added at 0 °C to a solution of InCl$_3$ (0.243 g, 1.1 mmol) in thf (5 cm^3). The reaction mixture was stirred for 2 h. The clear solution was filtered and the solvent removed. The residue was extracted with CH$_2$Cl$_2$ (20 cm^3), filtered again, and the solution concentrated to *ca.* 10 cm^3 under reduced pressure. Addition of hexane afforded first an unidentified yellow oil. White microcrystals precipitated at −30 °C, which were dried *in vacuo* (0.52 g, 60%) (Found: C, 41.90; H, 3.85. Calc. for C$_{68}$H$_{74}$Cl$_4$In$_2$Fe$_2$O$_{12}$P$_4$Si$_2$·2CH$_2$Cl$_2$: C, 41.45; H, 3.95). IR: ν(CO) (thf) 2023mw, 1972 (sh), 1955vs; (KBr) 2024m, 1970 (sh) and 1952vs cm^{-1}. FIR (polyethylene): ν(InCl) 330–250s (br) cm^{-1}. NMR: ^{1}H (200 MHz, CDCl$_3$), δ 1.0–2.5 (br m, 8 H, CH$_2$), 3.49 (s, 9 H, OCH$_3$) and 7.02–7.66 (m, 20 H, C$_6$H$_5$); ^{31}P-{^{1}H} (81.02 MHz, thf–C$_6$D$_6$), δ 49.0 [br s, P(Fe)] and −16.0 [br s, P(In)].

mer-[SnPh$_2${Fe(CO)$_3$[Si(OMe)$_3$](dppm-*P*)}$_2$] **16** *and mer,-cis*-[Fe(CO)$_3$(dppm-*P*)(SnClPh$_2$)$_2$] **17**.—A solution of K[Fe(CO)$_3${Si(OMe)$_3$}(dppm-*P*)] (0.685 g, 1.0 mmol) in thf (20 cm^3) was slowly added at 0 °C to a solution of SnCl$_2$Ph$_2$ (0.344 g, 1 mmol) in thf (10 cm^3). After stirring for several hours at room temperature the resulting yellow solution was filtered to remove KCl and the volume was reduced to 10 cm^3. Addition of an equivalent volume of hexane induced precipitation of the less-soluble white complex **16**. Slow diffusion of hexane into the solution afforded dichroic red-yellow crystals of **17** and a further crop of **16**. The two substances were separated by hand. Slow diffusion of hexane into a CH$_2$Cl$_2$ solution of **17** at 5 °C afforded bright yellow crystals, suitable for X-ray analysis. The ratio of **16**:**17** was found by ^{31}P-{^{1}H} spectroscopy to be 1:1. Complex **16** (Found: C, 54.35; H, 4.55. Calc. for C$_{74}$H$_{72}$Fe$_2$O$_{12}$P$_4$Si$_2$Sn: C, 56.85; H, 4.65%). IR (KBr): ν(CO) 2044s, 2003m and 1970vs cm^{-1}. NMR: ^{1}H (200 MHz, CDCl$_3$), δ 3.32 (s, 9 H, OCH$_3$), 3.49 (br s, 11 H, OCH$_3$, CH$_2$), 3.70 [d, CH$_2$, 2 H, ^2J(P–H) = 7] and 7.07–7.85 (m, 50 H, C$_6$H$_5$); ^{31}P-{^{1}H} (81.02 MHz, CH$_2$Cl$_2$–C$_6$D$_6$), δ 48.0 [d, P(Fe), ^2J(PP) = 55, ^2J(P–^{117,119}Sn) *ca.* 135], 42.7 [d, P(Fe), ^2J(PP) = 58, ^2J(P–^{117,119}Sn) *ca.* 135], −24.9 [d, ^2J(P–P) = 58] and −27.2 [d, ^2J(P–P) = 55 Hz].

Complex **17** (Found: C, 53.95; H, 4.20. Calc. for C$_{52}$H$_{42}$Cl$_2$FeO$_3$P$_2$Sn$_2$: C, 54.75; H, 3.70%). IR: ν(CO) (KBr) 2032s, 1989m, 1967 (sh), 1955vs; (CH$_2$Cl$_2$) 2038m, 1997m and 1970vs cm^{-1}. FIR (polyethylene): 360w, 294m, 270s, 259s, 248s, 240m and 211m cm^{-1}. NMR: ^{1}H (200 MHz, CDCl$_3$), δ 3.23 [d, CH$_2$, 2 H, ^2J(PH) = 8.2] and 6.9–7.8 (m, 40 H, C$_6$H$_5$); ^{31}P-{^{1}H} (81.02 MHz, CH$_2$Cl$_2$–C$_6$D$_6$), δ 47.5 [d, P(Fe), ^2J(PP) = 83, ^2J(P–^{117,119}Sn-*cis* = 121, ^2J(P–^{117,119}Sn-*trans*) = 157] and −26.7 [d, P(Sn), ^1J(P–^{117,119}Sn) = 85 Hz].

mer-[{[(MeO)$_3$Si](OC)$_3$Fe[μ-(Ph$_2$P)C$_5$H$_4$N]Zn(μ-Cl)}$_2$] **18**.—The synthesis was similar to that described for complex **3**, using **2d** (0.566 g, 1.0 mmol), ZnCl$_2$ (0.143 g, 1.05 mmol), colourless powder (0.582 g, 93%). No satisfactory microanalytical results could be obtained. IR: ν(CO) (thf) 1989m, 1928s, 1906vs; (CH$_2$Cl$_2$) 1989m, 1923s and 1903vs cm^{-1}. NMR: ^{1}H (200 MHz) (CDCl$_3$), δ 3.68 (br s, 9 H, OCH$_3$) and 6.78–9.10 (m, 14 H, C$_6$H$_5$, C$_5$H$_4$N); (CD$_2$Cl$_2$, 185 K), δ 3.52 (br s, 6 H, OCH$_3$) and 3.6 (br s, 3 H, OCH$_3$); ^{31}P-{^{1}H} (81.02 MHz, thf–C$_6$D$_6$), δ 88.6 [s, P(Fe)].

mer-[{[(MeO)$_3$Si](OC)$_3$Fe[μ-(Ph$_2$P)C$_5$H$_4$N]Zn(μ-I)}$_2$] **19**.—The synthesis was similar to that described for complex **3**, using K[Fe(CO)$_3${(Ph$_2$P)C$_5$H$_4$N}{Si(OMe)$_3$}] (0.566 g, 1.0 mmol) and ZnI$_2$ (0.335 g, 1.05 mmol), to give yellowish crystals (0.737 g, 92%) (Found: C, 34.55; H, 3.35; N, 1.55. Calc. for C$_{46}$H$_{46}$Fe$_2$I$_2$N$_2$O$_{12}$P$_2$Si$_2$Zn$_2$·2CH$_2$Cl$_2$: C, 35.95; H, 3.15; N, 1.75%). IR (thf): 1991m, 1929s, 1908vs [ν(CO)] and 1585w cm^{-1}. NMR: ^{1}H (200 MHz, CDCl$_3$), δ 3.69 (s, 9 H, OCH$_3$) and 7.26–9.42 (m, 14 H, C$_6$H$_5$, C$_5$H$_4$N); ^{31}P-{^{1}H} (81.02 MHz, thf–C$_6$D$_6$), δ 87.8 [s, P(Fe)].

mer-[{(MeO)$_3$Si}(OC)$_3$Fe{μ-(Ph$_2$P)C$_5$H$_4$N}ZnCl(4Me-py)] **20**.—To a solution of complex **18** (0.063 g, 0.05 mmol) in CH$_2$Cl$_2$ (5 cm^3) was added 4Me-py (9.5 μl, 0.1 mmol) *via* a microsyringe. The clear colourless solution was stirred for 5 min and the solvent removed under reduced pressure. The colourless residue was dried *in vacuo* for several hours (0.072 g, 99%) (Found: C, 44.70; H, 3.90; N, 3.65. Calc. for C$_{29}$H$_{30}$ClFeN$_2$O$_6$PSiZn·CH$_2$Cl$_2$: C, 44.85; H, 4.00; N, 3.50%). IR (CH$_2$Cl$_2$): 1987m, 1924s, 1900vs [ν(CO)], 1620m and 1587w cm^{-1}. FIR (polyethylene): 307w, 297w, 261s and 230m cm^{-1}. NMR: ^{1}H (200 MHz, CDCl$_3$), δ 2.40 (s, 3 H, CH$_3$), 3.67 (s, 9 H, OCH$_3$) and 7.18–8.89 (m, 18 H, C$_6$H$_5$, C$_5$H$_4$N); ^{31}P-{^{1}H} (81.02 MHz, thf–C$_6$D$_6$), δ 88.6 [s, P(Fe)].

mer-[{(MeO)$_3$Si}(OC)$_3$Fe{μ-(Ph$_2$P)C$_5$H$_4$N}ZnCl(Bu^{t}NC)] **21**.—To a solution of complex **18** (0.063 g, 0.05 mmol) in CH$_2$Cl$_2$ (5 cm^3) was added Bu^{t}NC (11 μl, 0.1 mmol) *via* a microsyringe. The resulting clear colourless solution was stirred for 5 min and the solvent removed under reduced pressure. The colourless residue was washed with hexane and dried *in vacuo* (0.079 g, 99%). The residue could be recrystallised by slow diffusion of hexane into a concentrated CH$_2$Cl$_2$ solution of it (Found: C, 43.80; H, 4.20; N, 3.60. Calc. for C$_{28}$H$_{32}$ClFeN$_2$O$_6$PSiZn·CH$_2$Cl$_2$: C, 43.90; H, 4.30; N, 3.55%). IR (KBr): 2219w [ν(NC)]; 1991m, 1936s, 1891vs [ν(CO)] and 1582w cm^{-1}. FIR (polyethylene): 293s, 277m, 242w, 209w, 181w and 117m cm^{-1}. NMR: ^{1}H (200 MHz, CDCl$_3$), δ 1.43 (s, 9 H, CH$_3$), 3.68 (s, 9 H, OCH$_3$) and 7.26–9.05 (m, 14 H, C$_6$H$_5$, C$_5$H$_4$N); ^{31}P-{^{1}H} (81.02 MHz, thf–C$_6$D$_6$), δ 88.7 [s, P(Fe)].

mer-[{(MeO)$_3$Si}(OC)$_3$Fe{μ-(Ph$_2$P)C$_5$H$_4$N}ZnEt] **22**.—To a cold solution of complex **1d** (0.525 g, 1.0 mmol) in diethyl ether (10 cm^3) a 1 mol dm^{-3} solution of ZnEt$_2$ in hexane was slowly added *via* a syringe (1 cm^3). A slight gas evolution was observed. The clear yellowish solution was evaporated to dryness under reduced pressure. The residue was washed with hexane (5 cm^3). (0.513 g, 83%). No satisfactory microanalytical results could be obtained. IR (CH$_2$Cl$_2$): 1985m, 1912 (sh), 1900vs [ν(CO)] and 1586w cm^{-1}. NMR: ^{1}H (200 MHz, C$_6$D$_6$), δ 1.06 [q, 2 H, CH$_2$, ^3J(HH) = 8 Hz], 1.77 (t, 3 H, CH$_3$), 3.97 (s, 9 H, OCH$_3$) and 6.36–8.23 (m, 14 H, C$_6$H$_5$, C$_5$H$_4$N).

mer-[{(MeO)Si}(OC)$_3$Fe{μ-(Ph$_2$P)C$_5$H$_4$N}GaCl$_2$] **23**.—A solution of complex **2d** (0.566 g, 1.0 mmol) in thf (20 cm^3) was added at 0 °C to a solution of GaCl$_3$ (0.194 g, 1.1 mmol) in thf (5 cm^3). The reaction mixture was stirred for 2 h. The clear solution was filtered and the solvent was removed. The residue was extracted with CH$_2$Cl$_2$ (20 cm^3), filtered again and the solution was concentrated to *ca.* 10 cm^3 under reduced pressure. Addition of hexane gave colourless microcrystals, which were dried *in vacuo* (0.610 g, 86%) (Found: C, 38.1; H, 2.9; N, 1.9. Calc. for C$_{23}$H$_{23}$Cl$_2$FeGaNO$_6$PSi·CH$_2$Cl$_2$: C, 38.45; H, 3.35; N, 1.85%). IR: (thf) 2036s, 1976s (sh), 1967s [ν(CO)] and 1589w; (KBr) 2032m, 1981 (sh), 1964vs and 1588w cm^{-1}. FIR (polyethylene): ν(GaCl) 347s cm^{-1}. NMR: ^{1}H (200 MHz, CD$_2$Cl$_2$), δ 3.71 (s, 9 H, OCH$_3$) and 7.28–9.36 (m, 14 H, C$_6$H$_5$, C$_5$H$_4$N); ^{31}P-{^{1}H} (81.02 MHz, CH$_2$Cl$_2$–C$_6$D$_6$), δ 82.9 [s, P(Fe)].

mer-[{(MeO)$_3$Si}(OC)$_3$Fe{μ-(Ph$_2$P)C$_5$H$_4$N}InCl$_2$] **24**.—The synthesis was similar to that described for complex **23**, using InCl$_3$ (0.243 g, 1.1 mmol) and **2d** (0.566 g, 1.0 mmol), to give colourless microcrystals (0.610 g, 86%) (Found: C, 39.2; H, 3.3; N, 2.1. Calc. for $C_{23}H_{23}Cl_2FeInNO_6PSi$: C, 38.90; H, 3.25; N, 1.95%). IR: (CH_2Cl_2) 2031s, 1976 (sh), 1959vs [ν(CO)] and 1584w; (KBr) 2049w, 2029m, 1973m, 1949vs [ν(CO)] and 1583w cm^{-1}. FIR (polyethylene): ν(InCl) 319s and 315 (sh) cm^{-1}. NMR: ^{1}H (200 MHz, CD_2Cl_2), δ 3.73 (s, 9 H, OCH_3) and 7.27–9.25 (m, 14 H, C_6H_5, C_5H_4N); ^{31}P-{^{1}H} (81.02 MHz, CH_2Cl_2–C_6D_6), δ 80.6 [s, P(Fe)].

mer-[{(MeO)$_3$Si}(OC)$_3$Fe{μ-(Ph$_2$P)C$_5$H$_4$N}Zn{W(C$_5$H$_5$)(CO)$_3$}] **26**.—Solid Na[W(C$_5$H$_5$)(CO)$_3$]·dme (0.650 g, 1.1 mmol) was added at 0 °C to a solution of *mer*-[{[(MeO)$_3$Si](OC)$_3$Fe[μ-(Ph$_2$P)C$_5$H$_4$N]Zn(μ-Cl)}$_2$] (0.362 g, 0.5 mmol) in thf (10 cm^3). The reaction mixture was stirred for 30 min at 0 °C, then filtered and the solvent removed. The residue was extracted with CH_2Cl_2 (20 cm^3), filtered again and the solution concentrated to *ca.* 5 cm^3 under reduced pressure. Addition of hexane afforded a colourless powder which was dried *in vacuo* (0.62 g, 67%) (Found: C, 38.60; H, 3.40; N, 1.55. Calc. for $C_{31}H_{28}FeNO_9PSiWZn$: C, 40.35; H, 3.05; N, 1.50%). NMR: ^{1}H (200 MHz, C_6D_6), δ 3.88 (s, 9 H, OCH_3), 5.32 (s, 5 H, C_5H_5) and 6.33–8.99 (m, 14 H, C_6H_5, C_5H_4N).

mer-[{(MeO)$_3$Si}(OC)$_3$Fe{μ-(Ph$_2$P)C$_5$H$_4$N}Cd{Mo(C$_5$H$_5$)(CO)$_3$}] **27**.—This compound was obtained at −20 °C by addition of Na[Mo(C$_5$H$_5$)(CO)$_3$]·dme to [{[(MeO)$_3$Si](OC)$_3$Fe[μ-(Ph$_2$P)C$_5$H$_4$N]Cd(μ-Br)}$_2$] or by addition of **2d** to [Mo(C$_5$H$_5$)(CO)$_3$(CdBr)]. At room temperature it decomposes in solution with formation of [Mo$_2$(C$_5$H$_5$)$_2$(CO)$_6$].

mer-[(OC)$_3${(MeO)$_3$Si}Fe{μ-(Ph$_2$P)C$_5$H$_4$N}Cd{W(C$_5$H$_5$)(CO)$_3$}] **28**.—The synthesis was similar to that described for complex **26**, using Na[W(C$_5$H$_5$)(CO)$_3$]·dme (0.650 g, 1.1 mmol) and *mer*-[{[(MeO)$_3$Si](OC)$_3$Fe[μ-(Ph$_2$P)C$_5$H$_4$N]Cd(μ-Br)}$_2$] (0.717 g, 0.5 mmol) at −20 °C to give a colourless powder (0.64 g, 66%) (Found: C, 38.25; H, 3.20; N, 1.25. Calc. for $C_{31}H_{28}CdFeNO_9PSiW$: C, 38.40; H, 2.90; N, 1.45%). NMR: ^{1}H (200 MHz, C_6D_6), δ 3.85 (s, 9 H, OCH_3), 5.11 (s, 5 H, C_5H_5) and 6.35–8.93 (m, 14 H, C_6H_5, C_5H_4N); ^{31}P-{^{1}H} (81.02 MHz, CH_2Cl_2–C_6D_6), δ 82.7 [s, P(Fe), ^{3+4}J(P–^{183}W) = 12, ^{2+3}J(P–^{111,113}Cd) = 63 Hz].

mer-[{(MeO)$_3$Si}(OC)$_3$Fe{μ-(Ph$_2$P)C$_5$H$_4$N}Hg{W(C$_5$H$_5$)(CO)$_3$}] **29**.—Solid [W(C$_5$H$_5$)(CO)$_3$(HgCl)] (0.295 g, 0.5 mmol) was added at 0 °C to a solution of K[Fe(CO)$_3${(Ph$_2$P)C$_5$H$_4$N}{Si(OMe)$_3$}] (0.283 g, 0.5 mmol) in thf (10 cm^3). The reaction mixture was stirred for 10 min, the solution was filtered and the solvent removed. The residue was extracted with CH_2Cl_2 (5 cm^3), filtered again and the solution concentrated. Addition of hexane afforded a yellow powder which was dried *in vacuo* (0.82 g, 70%) (Found: C, 32.40; H, 2.45; N, 1.05. Calc. for $C_{31}H_{28}FeHgNO_9PSiW\cdot CH_2Cl_2$: C, 33.65; H, 2.65; N, 1.25%). NMR: ^{1}H (200 MHz, C_6D_6), δ 3.84 (s, 9 H, OCH_3), 4.97 (s, 5 H, C_5H_5) and 6.45–8.98 (m, 14 H, C_6H_5, C_5H_4N); ^{31}P-{^{1}H} (81.02 MHz, CH_2Cl_2–C_6D_6), δ 70.7 [s, P(Fe), ^{2+3}J(P–^{199}Hg) = 170, ^{3+4}J(P–^{183}W) = 28 Hz].

mer-[{(MeO)$_3$Si}(OC)$_3$Fe{μ-(Ph$_2$P)C$_5$H$_4$N}InCl{W(C$_5$H$_5$)(CO)$_3$}] **30**.—Solid Na[W(C$_5$H$_5$)(CO)$_3$]·dme (0.650 g, 1.1 mmol) was added to a solution of complex **24** (0.710 g, 1 mmol) in thf (20 cm^3). The reaction mixture was stirred for 2 h; the solution was then filtered and the solvent removed. The residue was extracted with CH_2Cl_2 (20 cm^3), filtered again and the solution concentrated to *ca.* 5 cm^3 under reduced pressure. Addition of hexane afforded a yellow powder which was dried *in vacuo* (0.65 g, 65%) (Found: C, 35.55; H, 2.55; N, 1.45. Calc. for $C_{31}H_{28}ClFeInNO_9PSiW\cdot CH_2Cl_2$: C, 35.20; H, 2.75; N, 1.30%). FIR (polyethylene): 261m [ν(InCl)] and 166m cm^{-1}. NMR: ^{1}H (200 MHz, CD_2Cl_2), δ 3.73 (s, 9 H, OCH_3), 5.54 (s, 5 H, C_5H_5) and 7.24–9.22 (m, 14 H, C_6H_5, C_5H_4N); ^{31}P-{^{1}H} (81.02 MHz, CH_2Cl_2–C_6D_6), δ 80.6 [s, P(Fe), ^{3+4}J(P–^{183}W) = 10 Hz].

mer-[{(MeO)$_3$Si}(Ph$_3$P)(OC)$_3$FeInCl{(NC)Mn(C$_5$H$_4$Me)(CO)$_2$}] **31**.—Solid Na[Mn(C$_5$H$_4$Me)(CO)$_2$(CN)] (0.070 g, 0.29 mmol) in thf (20 cm^3) was added to a solution of complex **3** (0.200 g, 0.28 mmol) in thf (5 cm^3). The reaction mixture was stirred for 2 h; the air-sensitive solution was then filtered and the solvent removed. The residue was extracted with toluene (20 cm^3), filtered again and the solution concentrated to *ca.* 10 cm^3 under reduced pressure. Slow diffusion of hexane into the toluene solution at 5 °C afforded orange crystals (0.16 g, 65%) (Found: C, 44.7; H, 3.6; N, 1.9. Calc. for $C_{33}H_{31}ClFeInMnNO_8PSi$: C, 44.55; H, 3.50; N, 1.55%). IR: (thf) ν(CN) 2056m, ν(CO) 2026mw, 1971 (sh), 1955s, 1923vs, 1866vs; (KBr) ν(CN) 2030 (sh); ν(CO) 2025s, 1968vs, 1918vs and 1869vs cm^{-1}. FIR (polyethylene): 325w (br) and 260m (br) cm^{-1}. NMR: ^{1}H (200 MHz, CD_2Cl_2), δ 3.63 (s, 3 H, OCH_3), 3.75 (s, 6 H, OCH_3), 7.53 (br m, 15 H, C_6H_5); ill resolved resonances at δ 1.9 and 4.35 are assigned to the C_5H_5Me protons although their integration is much lower than expected; ^{31}P-{^{1}H} (81.02 MHz) (toluene–C_6D_6, 323 K), δ 54.5 [s, P(Fe)]; (thf–C_6D_6), 56.0 (br s, P(Fe)].

[(OC)$_2$(C$_5$H$_4$Me)Mn(CN)InCl$_2$] **32**.—Solid Na[Mn(C$_5$H$_4$Me)(CO)$_2$(CN)] (0.600 g, 2.5 mmol) was added to a suspension of $InCl_3$ (0.555 g, 2.5 mmol) in toluene (20 cm^3); thf (1 cm^3) was added and the slurry stirred for 2 h. The resulting mixture was filtered to remove NaCl and evaporated to dryness to yield a yellow, very air- and mixture-sensitive oil (0.8 g, 90%). No satisfactory microanalytical data could be obtained. IR (toluene): ν(CN) 2041m; ν(CO) 1922s and 1870s cm^{-1}. ^{1}H (NMR) (200 MHz, C_6D_6, 298 K): δ 1.5 (br, 3 H, CH_3) and 4.3 (br, 4 H, C_5H_4).

mer-[(OC)$_3$Fe{μ-Si(OMe)$_2$(OMe)}{μ-(Ph$_2$P)C$_5$H$_4$N}Zn{(NC)Mn(C$_5$H$_4$Me)(CO)$_2$}] **33**.—Solid Na[Mn(C$_5$H$_4$Me)(CO)$_2$(CN)] (0.240 g, 1.0 mmol) was added to a thf solution of complex **18** (0.625 g, 0.5 mmol) at 0 °C. The reaction mixture was stirred for 1 h, the solution filtered and the solvent removed. The residue was extracted with toluene (20 cm^3), filtered again and the solution concentrated to *ca.* 10 cm^3 under reduced pressure. Precipitation with hexane yielded a pale yellow powder (0.692 g, 86%). No satisfactory microanalysis could be obtained. IR: (thf) ν(CN) 2077m, ν(CO) 1988w, 1921vs, 1911 (sh) and 1859s; (toluene) ν(CN) 2068m, ν(CO) 1992m, 1920vs, 1910 (sh) and 1857s cm^{-1}. ^{31}P-{^{1}H} NMR: (81.02 MHz, CH_2Cl_2–C_6D_6) δ 87.6 [vbr, P(Fe)].

mer-[(OC)$_3$Fe{μ-Si(OMe)$_2$(OMe)}{μ-(Ph$_2$P)C$_5$H$_4$N}Cd{(NC)Mn(C$_5$H$_4$Me)(CO)$_2$}] **34**.—A synthesis similar to that described for complex **33** was used. The salt Na[Mn(C$_5$H$_4$Me)(CO)$_2$(CN)] (0.240 g, 1.0 mmol) and *mer*-[{(MeO)$_3$Si](OC)$_3$Fe[μ-(Ph$_2$P)C$_5$H$_4$N]Cd(μ-Br)}$_2$] (0.717 g, 0.5 mmol) in thf (5 cm^3) gave a colourless powder (0.53 g, 62%) (Found: C, 45.50; H, 3.65; N, 3.75. Calc. for $C_{32}H_{30}CdFeMnNO_8PSi$: C, 45.05; H, 3.55; N, 3.30%). IR: (thf) ν(CN) 2064m, ν(CO) 1989m, 1920vs, 1911 (sh) and 1858s; (toluene) ν(CN) 2060m, ν(CO) 1991m, 1919vs, 1911 (sh) and 1857s cm^{-1}. NMR: ^{1}H (200 MHz), see text; ^{31}P-{^{1}H} (81.02 MHz, CH_2Cl_2–C_6D_6), δ 85.4 [s, P(Fe), ^2J(P–^{111,113}Cd) = 87 Hz].

Crystal Structure Determinations.—Suitable single crystals of complexes **6**, **12** and **17** were obtained by slow diffusion of hexane into PhCl (**6** and **12**) or CH_2Cl_2 (**17**) solutions at 5 °C. For each compound a single crystal was cut from a cluster of crystals and mounted on a rotation-free goniometer head. Systematic searches in reciprocal space showed that crystals of **12**·PhCl belong to the triclinic system, whereas those of **6**·PhCl and **17**·CH_2Cl_2 belong to the monoclinic system.

Quantitative data were obtained at room temperature. All experimental parameters used are given in Table 6. The resulting data sets were transferred to a VAX computer, and for all subsequent calculations the Enraf-Nonius SDP/VAX

Table 6 X-Ray experimental data for complexes **6**, **12** and **17** *

	6·PhCl	12·PhCl	17·CH_2Cl_2
Formula	$C_{48}H_{44}Cl_3FeInO_7P_2Si$	$C_{46}H_{43}Cl_2FeInMoO_9P_2Si$	$C_{53}H_{44}Cl_4FeO_3P_2Sr_2$
M	1099.9	1167.4	1225.9
Crystal system	Monoclinic	Triclinic	Monoclinic
Space group	$P2_1/c$	$P\bar{1}$	$P2_1/c$
a/Å	12.500(3)	10.785(3)	17.467(5)
b/Å	11.214(3)	12.141(3)	11.896(3)
c/Å	34.871(10)	21.028(6)	24.448(7)
α/°		98.17(2)	
β/°	99.61(2)	96.09(2)	90.62(2)
γ/°		114.42(2)	
U/Å^3	4819.5	2439.8	5079.5
Z	4	2	4
D_c/g cm^{-3}	1.516	1.589	1.603
μ/cm^{-1}	10.771	12.516	15.769
F(000)	2232	1172	2440
Crystal dimensions (mm)	0.30 × 0.20 × 0.10	0.20 × 0.30 × 0.30	0.12 × 0.30 × 0.32
Scan width/°	0.70 + 0.34 tanθ	1.05 + 0.34 tanθ	1.05 + 0.34 tanθ
Octants	$\pm h + k + l$	$\pm h \pm k + l$	$\pm h + k + l$
θ_{min}, θ_{max}/°	2, 22	2, 24	2, 24
Number of data collected	6786	8557	10 264
Number of data with $I > 3\sigma(I)$	4461	6686	4428
Minimum, maximum absorption	0.93, 1.00	0.95, 1.00	0.94, 1.00
R	0.048	0.045	0.037
R'	0.076	0.070	0.056
p	0.08	0.08	0.08
Goodness of fit	1.687	1.550	1.161

* Details in common: yellow; monochromated Mo-Kα radiation (λ 0.7107 Å); Enraf-Nonius CAD4-F diffractometer; 20 °C; θ–2θ scans; variable scan speed.

Table 7 Positional parameters and their e.s.d.s for complex **6**

Atom	*x*	*y*	*z*	Atom	*x*	*y*	*z*
In	0.7555 59(4)	0.128 47(5)	0.372 45(1)	C(21)	1.136 3(7)	0.015 5(8)	0.363 1(2)
Cl(1)	0.577 5(2)	0.196 4(2)	0.342 60(6)	C(22)	1.237 6(7)	0.059 7(9)	0.359 2(3)
Cl(2)	0.224 0(2)	0.074 6(2)	0.645 96(7)	C(23)	1.269 1(7)	0.169(1)	0.372 6(2)
Fe	0.856 90(8)	0.211 99(9)	0.438 12(3)	C(24)	1.200 6(6)	0.237 4(8)	0.390 5(3)
C(1)	0.775 7(6)	0.333 5(7)	0.417 7(2)	P(2)	0.193 3(2)	−0.234 7(2)	0.719 61(6)
O(1)	0.724 2(4)	0.413 6(5)	0.405 3(2)	O(7)	0.174 5(4)	−0.198 7(5)	0.677 6(1)
C(2)	0.888 4(6)	0.261 9(7)	0.486 2(2)	C(25)	0.253 8(6)	−0.119 2(7)	0.752 0(2)
O(2)	0.907 5(5)	0.294 9(6)	0.517 8(2)	C(26)	0.335 0(6)	−0.048 5(8)	0.741 5(2)
C(3)	0.907 8(6)	0.062 9(7)	0.445 5(2)	C(27)	0.381 0(6)	0.042 2(8)	0.766 5(3)
O(3)	0.941 8(5)	−0.030 6(5)	0.451 2(2)	C(28)	0.343 6(7)	0.063 8(9)	0.801 0(3)
Si	0.704 6(2)	0.137 5(2)	0.459 40(6)	C(29)	0.263 3(7)	−0.003(1)	0.811 2(3)
O(4)	0.626 9(5)	0.242 5(6)	0.470 0(2)	C(30)	0.218 0(7)	−0.096 9(9)	0.786 8(2)
C(4)	0.525(1)	0.238(1)	0.480 9(4)	C(31)	0.275 2(6)	−0.368 7(8)	0.729 2(2)
O(5)	0.724 0(5)	0.041 0(6)	0.495 2(2)	C(32)	0.270 5(7)	−0.453 3(8)	0.700 3(3)
C(5)	0.742(1)	0.054(1)	0.534 8(3)	C(33)	0.320 6(7)	−0.560 9(9)	0.708 6(3)
O(6)	0.644 0(4)	0.053 5(6)	0.423 7(2)	C(34)	0.377 4(7)	−0.584(1)	0.743 7(4)
C(6)	0.551 3(8)	−0.019(1)	0.422 4(4)	C(35)	0.385 2(7)	−0.501(1)	0.772 3(3)
P(1)	1.012 9(1)	0.286 5(2)	0.41 95(5)	C(36)	0.334 6(7)	−0.390 3(9)	0.765 9(3)
C(7)	1.114 8(5)	0.318 9(7)	0.465 4(2)	C(37)	0.064 8(5)	−0.265 9(7)	0.735 1(2)
C(8)	1.144 0(7)	0.229 2(7)	0.491 4(2)	C(38)	−0.021 0(6)	−0.195 2(7)	0.720 9(2)
C(9)	1.224 0(7)	0.246 7(8)	0.523 8(3)	C(39)	−0.119 4(6)	−0.208 5(8)	0.733 8(3)
C(10)	1.273 9(7)	0.353 5(9)	0.530 4(3)	C(40)	−0.127 6(6)	−0.295 0(8)	0.761 4(2)
C(11)	1.245 2(7)	0.443 2(8)	0.504 3(3)	C(41)	−0.044 2(6)	−0.367 5(8)	0.774 9(3)
C(12)	1.168 1(7)	0.427 8(8)	0.472 5(2)	C(42)	0.052 5(6)	−0.354 6(8)	0.761 6(2)
C(13)	0.993 1(5)	0.428 1(7)	0.395 4(2)	C(43)	0.540 9(5)	0.331 1(7)	0.627 2(2)
C(14)	0.956 2(7)	0.525 7(7)	0.414 5(2)	C(44)	0.494 4(5)	0.442 3(7)	0.618 2(2)
C(15)	0.936 2(7)	0.633 2(7)	0.395 5(3)	C(45)	0.534 8(5)	0.516 1(7)	0.593 1(2)
C(16)	0.951 6(7)	0.642 3(8)	0.357 2(3)	C(46)	0.618 0(5)	0.476 5(7)	0.574 6(2)
C(17)	0.987 6(7)	0.546 4(8)	0.338 4(2)	C(47)	0.673 7(5)	0.372 6(7)	0.587 2(2)
C(18)	1.008 0(6)	0.439 3(7)	0.357 6(2)	C(48)	0.629 3(5)	0.296 1(7)	0.610 5(2)
C(19)	1.093 8(6)	0.196 5(7)	0.394 6(2)	Cl(3)	0.497 5(5)	0.231 8(6)	0.656 8(2)
C(20)	1.066 5(6)	0.084 1(7)	0.380 4(2)				

package[40] was used. Three standard reflections measured every hour during the entire data collection showed no significant trends. The raw data were converted into intensities and corrected for Lorentz, polarisation and absorption factors, the latter computed from ψ scans of four reflections. The structures were solved using the heavy-atom method. After refinement of the heavy atoms, Fourier difference maps revealed maxima of residual electronic density close to the positions expected for hydrogen atoms; they were introduced in structure-factor calculations by their computed coordinates (C–H 0.95 Å) and

Table 8 Positional parameters and their e.s.d.s for complex **12**

Atom	*x*	*y*	*z*
In	0.232 46(3)	0.333 44(3)	0.238 09(2)
P(1)	0.166 8(1)	0.497 5(1)	0.317 37(6)
P(2)	0.309 1(1)	0.650 16(9)	0.219 71(6)
C(1)	0.156 6(4)	0.593 6(4)	0.259 0(2)
C(2)	0.293 2(5)	0.603 3(4)	0.387 9(2)
C(3)	0.294 1(6)	0.715 1(5)	0.413 8(3)
C(4)	0.391 3(8)	0.793 8(6)	0.467 6(3)
C(5)	0.485 5(7)	0.762 4(8)	0.496 0(3)
C(6)	0.486 7(7)	0.650 9(8)	0.471 4(4)
C(7)	0.390 8(6)	0.572 8(6)	0.417 3(3)
C(8)	−0.000 8(5)	0.447 7(4)	0.343 9(2)
C(9)	−0.007 2(6)	0.425 5(6)	0.406 1(3)
C(10)	−0.134 3(7)	0.385 3(7)	0.427 4(3)
C(11)	−0.251 4(6)	0.366 8(5)	0.387 7(3)
C(12)	−0.245 6(6)	0.385 0(6)	0.325 8(3)
C(13)	−0.121 0(6)	0.423 6(6)	0.303 3(3)
C(14)	0.247 7(5)	0.699 1(4)	0.148 9(2)
C(15)	0.337 2(6)	0.805 8(5)	0.130 5(3)
C(16)	0.295 5(8)	0.838 0(5)	0.073 9(3)
C(17)	0.168 2(7)	0.765 5(6)	0.036 2(3)
C(18)	0.082 4(6)	0.661 3(6)	0.053 9(3)
C(19)	0.120 5(5)	0.628 1(5)	0.110 8(3)
C(20)	0.423 7(5)	0.797 4(4)	0.273 9(2)
C(21)	0.376 2(6)	0.887 2(5)	0.288 8(3)
C(22)	0.465 1(8)	1.001 3(5)	0.330 4(3)
C(23)	0.597 9(8)	1.024 5(6)	0.355 9(4)
C(24)	0.646 7(7)	0.938 0(6)	0.341 3(4)
C(25)	0.559 5(6)	0.824 8(5)	0.300 1(3)
Mo	−0.019 09(4)	0.121 94(4)	0.180 32(2)
C(26)	−0.092 3(7)	−0.032 8(6)	0.087 5(3)
C(27)	0.025 8(7)	0.067 6(6)	0.078 3(3)
C(28)	0.135 8(6)	0.081 7(6)	0.123 4(4)
C(29)	0.086 8(7)	−0.008 6(6)	0.162 5(4)
C(30)	−0.053 5(7)	−0.007 3(5)	0.139 5(4)
C(31)	−0.237 1(9)	−0.089 7(8)	0.043 1(4)
C(32)	−0.001 4(6)	0.146 9(5)	0.276 6(3)
O(1)	0.000 4(5)	0.154 8(5)	0.331 6(2)
C(33)	−0.044 0(5)	0.264 7(5)	0.159 8(3)
O(2)	−0.064 5(4)	0.343 1(3)	0.143 7(2)
C(34)	−0.213 7(6)	0.069 3(5)	0.189 3(3)
O(3)	−0.328 8(4)	0.036 6(4)	0.193 6(3)
Fe	0.401 11(6)	0.519 58(5)	0.188 42(3)
C(35)	0.521 3(5)	0.638 4(4)	0.156 8(3)
O(4)	0.600 3(4)	0.716 2(4)	0.136 4(2)
C(36)	0.272 8(5)	0.431 9(4)	0.117 5(2)
O(5)	0.194 0(4)	0.376 1(4)	0.070 6(2)
C(37)	0.505 1(4)	0.535 6(4)	0.264 6(2)
O(6)	0.575 5(4)	0.548 8(3)	0.311 7(2)
Si	0.514 4(1)	0.407 1(1)	0.148 87(8)
O(7)	0.679 8(4)	0.465 6(4)	0.177 8(2)
C(38)	0.786 2(8)	0.562 8(9)	0.168 2(7)
O(8)	0.497 4(5)	0.386 0(5)	0.071 1(2)
C(39)	0.575(2)	0.363(2)	0.029 6(6)
O(9)	0.451 8(4)	0.273 4(3)	0.170 7(3)
C(40)	0.514 4(7)	0.189 9(6)	0.170 0(6)
Cl(1)	0.346 9(2)	0.268 6(1)	0.322 33(8)
C(41)	0.997 8(9)	0.839 8(8)	0.375 8(5)
C(42)	0.908(1)	0.747 0(9)	0.400 8(6)
C(43)	0.942(1)	0.759(1)	0.466 4(7)
C(44)	1.043(1)	0.854(1)	0.505 5(5)
C(45)	1.133(1)	0.952(1)	0.476 9(6)
C(46)	1.110(1)	0.944 3(9)	0.413 0(6)
Cl(2)	0.972 3(5)	0.837 7(4)	0.294 3(2)

Table 9 Positional parameters and their e.s.d.s for complex **17**

Atom	*x*	*y*	*z*
Sn(1)	0.819 44(3)	0.164 00(5)	0.167 85(2)
Sn(2)	0.690 42(3)	0.297 94(5)	0.655 59(2)
Fe	0.808 77(6)	0.164 67(9)	0.061 55(4)
Cl(1)	0.957 8(1)	0.152 9(3)	0.181 0(1)
Cl(2)	0.637 3(1)	0.216 9(2)	0.152 1(1)
P(1)	0.817 0(1)	0.151 3(2)	−0.030 81(8)
P(2)	0.733 0(1)	0.371 5(2)	−0.053 59(9)
O(1)	0.936 9(3)	0.007 1(5)	0.064 5(3)
O(2)	0.697 0(3)	−0.016 9(5)	0.075 9(3)
O(3)	0.886 2(3)	0.380 7(5)	0.078 8(2)
C(1)	0.889 0(5)	0.068 2(7)	0.064 6(3)
C(2)	0.739 0(4)	0.054 6(7)	0.069 6(3)
C(3)	0.856 6(4)	0.296 9(7)	0.071 5(3)
C(4)	0.745 3(4)	0.225 3(6)	−0.073 4(3)
C(5)	0.907 7(4)	0.192 8(6)	−0.060 5(3)
C(6)	0.970 1(4)	0.226 1(7)	−0.028 6(3)
C(7)	1.038 1(5)	0.261 6(8)	−0.054 4(4)
C(8)	1.045 3(5)	0.264 4(9)	−0.109 4(4)
C(9)	0.983 8(5)	0.231(1)	−0.140 1(4)
C(10)	0.916 4(5)	0.194 5(8)	−0.116 2(4)
C(11)	0.806 4(4)	0.006 7(6)	−0.054 4(3)
C(12)	0.870 3(5)	−0.057 7(7)	−0.068 3(4)
C(13)	0.861 4(6)	−0.168 1(7)	−0.084 9(4)
C(14)	0.791 2(6)	−0.216 1(7)	−0.088 0(4)
C(15)	0.728 7(6)	−0.156 5(8)	−0.074 9(5)
C(16)	0.736 5(5)	−0.043 2(7)	−0.057 7(4)
C(17)	0.815 8(4)	0.440 8(6)	−0.083 5(3)
C(18)	0.870 0(5)	0.488 4(7)	−0.048 9(3)
C(19)	0.935 8(5)	0.537 7(8)	−0.073 2(4)
C(20)	0.945 6(5)	0.539 1(8)	−0.127 7(4)
C(21)	0.891 6(5)	0.494 3(9)	−0.160 5(4)
C(22)	0.828 1(5)	0.444 4(8)	−0.139 2(4)
C(23)	0.656 1(4)	0.423 4(7)	−0.096 4(4)
C(24)	0.633 3(5)	0.532 1(8)	−0.089 7(4)
C(25)	0.572 5(6)	0.576(1)	−0.118 5(5)
C(26)	0.535 0(6)	0.512(1)	−0.155 9(5)
C(27)	0.556 4(6)	0.406(1)	−0.167 1(6)
C(28)	0.618 6(5)	0.359(1)	−0.134 5(5)
C(29)	0.790 3(5)	0.007 8(7)	0.206 6(3)
C(30)	0.720 6(6)	−0.007 8(8)	0.233 0(4)
C(31)	0.706 5(6)	−0.109 1(9)	0.260 4(4)
C(32)	0.758 2(8)	−0.191 8(9)	0.261 1(4)
C(33)	0.827 3(8)	−0.177 7(9)	0.234 4(5)
C(34)	0.842 2(6)	−0.079 9(8)	0.206 8(4)
C(35)	0.807 5(5)	0.306 8(7)	0.220 7(3)
C(36)	0.744 1(6)	0.321 7(8)	0.255 1(4)
C(37)	0.737 8(6)	0.410 4(9)	0.289 9(4)
C(38)	0.792 5(8)	0.488 9(9)	0.291 6(4)
C(39)	0.857 6(8)	0.481 8(9)	0.258 6(5)
C(40)	0.864 8(6)	0.388 4(9)	0.222 3(4)
C(41)	0.585 7(4)	0.264 8(7)	0.021 3(4)
C(42)	0.542 2(5)	0.348 5(7)	0.000 6(4)
C(43)	0.474 3(5)	0.328 2(8)	−0.027 1(4)
C(44)	0.448 9(5)	0.226 4(9)	−0.034 1(5)
C(45)	0.492 1(8)	0.143(1)	−0.017 0(8)
C(46)	0.560 6(6)	0.160 3(9)	0.012 2(6)
C(47)	0.699 0(4)	0.470 2(7)	0.092 0(3)
C(48)	0.728 8(5)	0.554 9(7)	0.060 7(4)
C(49)	0.734 3(5)	0.664 7(8)	0.079 2(4)
C(50)	0.708 9(6)	0.692 0(8)	0.129 1(5)
C(51)	0.679 8(7)	0.612(1)	0.162 2(5)
C(52)	0.675 2(6)	0.498 3(8)	0.144 4(4)
C(53)	0.466(1)	−0.057(3)	0.140(1)
Cl(3)	0.434 5(6)	0.102(1)	0.183 6(5)
Cl(4)	0.489 6(7)	−0.101(1)	0.199 8(6)

isotropic thermal parameters such as $B(\mathrm{H}) = 1.3\,B_{\mathrm{eq}}(\mathrm{C})$ Å^2 but not refined. The solvent hydrogen atoms for complex **17** were omitted. Full least-squares refinements; weighting scheme $w = 1/\sigma^2(F)$ $\sigma^2(F^2) = \sigma^2_{\mathrm{counts}} + (pI)^2$. A final difference map revealed no significant maxima. The scattering factor coefficients and anomalous dispersion coefficients were from ref. 41. Final atomic coordinates are given in Tables 7–9. Structures were drawn with the program ORTEP.[42]

Additional material available from the Cambridge Crystallographic Data Centre comprises H-atom coordinates, thermal parameters and remaining bond lengths and angles.

Acknowledgements

Financial support from the Centre National de la Recherche Scientifique (Paris) and the Commission of the European Communities (Contract No. ST2J-0479) is gratefully acknowledged.

References

1 (*a*) M. J. Mays and J. D. Robb, *J. Chem. Soc. A*, 1968, 329; (*b*) M. J. Mays and J. D. Robb *J. Chem. Soc. A*, 1969, 561; (*c*) J. M. Burlitch and A. Ferrari, *Inorg. Chem.*, 1970, **9**, 563; (*d*) A. T. T. Hsieh, *Inorg. Chim. Acta*, 1975, **14**, 87.

2 (*a*) J. M. Burlitch, in *Comprehensive Organometallic Chemistry*, eds. G. Wilkinson, F. G. A. Stone and E. W. Abel, Pergamon, Oxford, 1982, vol. 6, p. 983; (*b*) S. Alvarez, M. Ferrer, R. Reina, O. Rossell, M. Seco and X. Solans, *J. Organomet. Chem.*, 1989, **377**, 291.

3 (*a*) P. Braunstein, M. Knorr, A. Tiripicchio and M. Tiripicchio-Camellini, *Angew. Chem., Int. Ed. Engl.*, 1989, **28**, 1361; (*b*) P. Braunstein, M. Knorr, E. Villarroya and J. Fischer, *New J. Chem.*, 1990, **14**, 583; (*c*) P. Braunstein, M. Knorr, H. Piana and U. Schubert, *Organometallics*, 1991, **10**, 828; (*d*) P. Braunstein, M. Knorr, E. Villarroya, A. DeCian and J. Fischer, *Organometallics*, 1991, **10**, 3714; (*e*) P. Braunstein, M. Knorr, U. Schubert, M. Lanfranchi and A. Tiripicchio, *J. Chem. Soc., Dalton Trans.*, 1991, 1507; (*f*) P. Braunstein, L. Douce, M. Knorr, M. Strampfer, M. Lanfranchi and A. Tiripicchio, *J. Chem. Soc., Dalton Trans.*, 1992, 331; (*g*) P. Braunstein, E. Colomer, M. Knorr, A. Tiripicchio and M. Tiripicchio-Camellini, *J. Chem. Soc., Dalton Trans.*, 1992, 903; (*h*) G. Reinhard, B. Hirle, U. Schubert, M. Knorr, P. Braunstein, A. DeCian and J. Fischer, *Inorg. Chem.*, 1993, **32**, 1656; (*i*) F. Balegroune, P. Braunstein, L. Douce, T. Dusausoy, D. Grandjean, M. Knorr and M. Strampfer, *J. Cluster Sci.*, 1992, **3**, 275; (*j*) M. Knorr and P. Braunstein, *Bull. Soc. Chim. Fr.*, 1992, **129**, 663; (*k*) P. Braunstein, M. Knorr, A. Tiripicchio and M. Tiripicchio Camellini, *Inorg. Chem.*, 1992, **36**, 3685; (*l*) G. Reinhard, B. Hirle and U. Schubert, *J. Organomet. Chem.*, 1992, **427**, 173; (*m*) P. Braunstein, in *Perspectives in Coordination Chemistry*, eds. A. F. Williams, C. Floriani and A. E. Merbach, Verlag Helvetica Chima Acta/VCH, Basle, 1992, pp. 67–107.

4 A. H. Cowley and R. A. Jones, *Angew Chem., Int. Ed. Engl.*, 1989, **28**, 1208.

5 *Chemical Perspectives of Microelectronics*, eds. M. E. Grass, J. M. Jasinski and T. Yates, *Mater. Res. Soc. Symp. Proc.*, 1989, **131**; *Ternary and Multinary Compounds*, eds. S. K. Deb and A. Zunger, Material Research Society, Pittsburgh, PA, 1987; R. A. Reynolds, *J. Vac. Sci. Technol.*, 1989, **A7**, 289.

6 (*a*) A. T. T. Hsieh and M. J. Mays, *J. Organomet. Chem.*, 1972, **37**, 9; (*b*) A. T. T. Hsieh and M. J. Mays, *J. Chem. Soc., Dalton Trans.*, 1972, 516; (*c*) J. Chatt, C. Eaborn and P. N. Kapoor, *J. Organomet. Chem.*, 1970, **23**, 109.

7 (*a*) L. M. Clarkson, W. Clegg, N. C. Norman, A. J. Tucker and P. M. Webster, *Inorg. Chem.*, 1988, **27**, 2653; (*b*) N. A. Compton, R. J. Errington and N. C. Norman, *Adv. Organomet. Chem.*, 1990, **31**, 91; (*c*) J. Weidlein, *Gmelin Handbook of Inorganic Chemistry, Organoindium Compounds*, ed. W. Petz, 8th edn., Springer, Berlin, 1991; (*d*) L. M. Clarkson, W. Clegg, D. C. R. Hockless, N. C. Norman and T. B. Marder, *J. Chem. Soc., Dalton Trans.*, 1991, 2229; (*e*) L. M. Clarkson, W. Clegg, D. C. R. Hockless, N. C. Norman, L. J. Farrugia, S. G. Bott and J. L. Atwood, *J. Chem. Soc., Dalton Trans.*, 1991, 2241; (*f*) L. M. Clarkson, N. C. Norman and L. J. Farrugia, *Organometallics*, 1991, **10**, 1286; (*g*) J. T. Leman, J. W. Ziller and A. R. Barron, *Organometallics*, 1991, **10**, 1766; (*h*) V. G. Albano, M. Cané, M. C. Iapalucci, G. Longoni and M. Monari, *J. Organomet. Chem.*, 1991, **407**, C9; (*i*) J. C. Calabrese, L. M. Clarkson, T. B. Marder, N. C. Norman and N. J. Taylor, *J. Chem. Soc., Dalton Trans.*, 1992, 3525; (*j*) M. Schollenberger, B. Nuber and M. L. Ziegler, *Angew. Chem., Int. Ed. Engl.*, 1992, **31**, 350; (*k*) R. A. Fischer, J. Behm, T. Priermeier and W. Scherer, *Angew. Chem., Int. Ed. Engl.*, 1993, **32**, 746.

8 (*a*) J.-C. Maire, U. Krüerke, M. Mirbach, W. Petz and C. Siebert, *Gmelin Handbook of Inorganic Chemistry, Organogallium Compounds*, eds. U. Krüerke, M. Mirbach, W. Petz and C. Siebert, 8th edn., Springer, Berlin, 1991; (*b*) R. A. Fischer and J. Behm, *J. Organomet. Chem.*, 1991, **431**, C10; (*c*) R. A. Fischer and J. Behm, *Chem. Ber.*, 1992, **125**, 37; (*d*) R. M. Campbell, L. M. Clarkson, W. Clegg, D. C. R. Hockless, N. L. Pickett and N. C. Norman, *Chem. Ber.*, 1992, **125**, 55; (*e*) R. Fischer, S. Scherer and M. Kleine, *Angew. Chem., Int. Ed. Engl.*, 1993, **32**, 748; (*f*) J. A. Zubieta and J. J. Zuckerman, *Prog. Inorg. Chem.*, 1978, **24**, 251; (*g*) A. G. Davies and P. J. Smith, in *Comprehensive Organometallic Chemistry*, eds. G. Wilkinson, F. G. A. Stone and E. W. Abel, Pergamon, Oxford, 1982.

9 H.-J. Haupt, W. Wolfes and H. Preut, *Inorg. Chem.*, 1976, **15**, 2920; (*b*) B. Neumüller, *Chem. Ber.*, 1989, **122**, 2283; A. J. Carty and D. G. Tuck, *Prog. Inorg. Chem.*, 1975, **19**, 243; D. H. Brown and D. T. Stewart, *J. Inorg. Nucl. Chem.*, 1970, **32**, 3751.

10 N. W. Alcock, I. A. Degnan, O. W. Howarth and M. G. H. Wallbridge, *J. Chem. Soc., Dalton Trans.*, 1992, 2775; I. A. Degnan, N. W. Alcock, S. M. Roe and M. G. H. Wallbridge, *Acta Crystallogr., Sect. C*, 1992, **48**, 995.

11 See H. Günther, *NMR Spektroskopie*, Georg Thieme, Stuttgart, 1983, ch. 8.

12 T. A. Albright, W. J. Freeman and E. E. Schweizer, *J. Org. Chem.*, 1975, **40**, 3437.

13 M. C. Ball and A. H. Norbury, in *Physical Data for Inorganic Chemists*, Longman, London, 1974.

14 A. Mitschler, B. Rees and M. S. Lehmann, *J. Am. Chem. Soc.*, 1978, **100**, 3390.

15 D. G. Tuck, in *Comprehensive Organometallic Chemistry*, eds. G. Wilkinson, F. G. A. Stone and E. W. Abel, Pergamon, Oxford, 1982, vol. 1, p. 683.

16 N. Wiberg, in *Holleman-Wiberg, Lehrbuch der Anorganischen Chemie*, 33rd edn., Walter de Gruyter, Berlin, 1985.

17 (*a*) M. Veith and J. Hans, *Angew Chem., Int. Ed. Engl.*, 1991, **30**, 878; (*b*) S. S. Al-Juaid, C. Eaborn, A. Habtemariam, P. B. Hitchcock and J. D. Smith, *J. Organomet. Chem.*, 1992, **437**, 41; (*c*) M. Veith, *Adv. Organomet. Chem.*, 1990, **31**, 269; (*d*) H. Tobita, K. Ueno, M. Shimoi and H. Ogino, *J. Am. Chem. Soc.*, 1990, **112**, 3415.

18 W. T. Robinson, C. J. Wilkins and Z. Zeying, *J. Chem. Soc., Dalton Trans.*, 1990, 219.

19 N. Burford, B. W. Royan, R. E. v. H. Spence, T. S. Cameron, A. Linden and R. D. Rogers, *J. Chem. Soc., Dalton Trans.*, 1990, 1521.

20 G. Ruben and V. Zabel, *Cryst. Struct. Commun.*, 1976, **5**, 671.

21 E. Kunz and U. Schubert, *Chem. Ber.*, 1989, **122**, 231.

22 O. T. Beachley, jun., M. A. Banks, M. R. Churchill, W. G. Feighery and J. C. Fettinger, *Organometallics*, 1991, **10**, 3036.

23 H. Preut and H. J. Haupt, *Acta Crystallogr., Sect. B*, 1979, **35**, 2191.

24 P. S. Pregosin and R. W. Kunz, *NMR Basic Principles and Progress*, eds. P. Diehl, E. Fluck and R. Kosfeld, Springer, Berlin, 1976, vol 16, p. 104.

25 M. Knorr, H. Piana, S. Gilbert and U. Schubert, *J. Organomet. Chem.*, 1990, **388**, 327.

26 P. Braunstein, M. Knorr, M. Strampfer, A. Tiripicchio and F. Ugozzoli, unpublished work.

27 N. Dominelli, E. Wood, P. Vasudev and C. H. W. Jones, *Inorg. Nucl. Chem. Lett.*, 1972, **8**, 1077.

28 B. J. Aylett, *Adv. Inorg. Chem. Radiochem.*, 1982, **25**, 1 and refs. therein.

29 (*a*) S. A. R. Knox and F. G. A. Stone, *J. Chem. Soc. A*, 1969, 2559; (*b*) J. R. Chipperfield, A. C. Hayter and D. E. Webster, *J. Chem. Soc., Dalton Trans.*, 1977, 921.

30 W. Davies and F. G. Mann, *J. Chem. Soc.*, 1944, 276; F. G. Mann and J. Watson, *J. Org. Chem.*, 1948, **13**, 502.

31 J. P. Farr, M. M. Olmstead and A. L. Balch, *J. Am. Chem. Soc.*, 1980, **102**, 6654; J. P. Farr, M. M. Olmstead, C. H. Hunt and A. L. Balch, *Inorg. Chem.*, 1981, **20**, 1182; A. Maisonnat, J. P. Farr and A. L. Balch, *Inorg. Chim. Acta*, 1981, **53**, L217; A. Maisonnat, J. P. Farr, M. M. Olmstead, C. T. Hunt and A. L. Balch, *Inorg. Chem.*, 1982, **21**, 3961.

32 F. I. Aigbirhio, S. S. Al-Juaid, C. Eaborn, A. Habtemariam, P. B. Hitchcock and J. D. Smith, *J. Organomet. Chem.*, 1991, **405**, 149.

33 C. G. Arena, E. Rotondo, F. Faraone, M. Lanfranchi and A. Tiripicchio, *Organometallics*, 1991, **10**, 3877.

34 D. L. Thorn, *J. Organomet. Chem.*, 1991, **405**, 161.

35 (*a*) H. Behrens, H.-D. Feilner, E. Lindner and D. Uhlig, *Z. Naturforsch., Teil B*, 1971, **26**, 990; (*b*) C. G. Pierpont, B. A. Sosinsky and R. G. Shong, *Inorg. Chem.*, 1982, **21**, 3247; (*c*) B. A. Sosinsky, R. G. Shong, B. J. Fitzgerald, N. Norem and C. O'Rourke, *Inorg. Chem.*, 1983, **22**, 3124.

36 J. M. Burlitch, *J. Am. Chem. Soc.*, 1969, **91**, 4562, 4563.

37 W. F. McNamara, E. N. Duesler and R. T. Paine, *Organometallics*, 1988, **7**, 384 and refs. therein.

38 P. Braunstein, B. Oswald, A. Tiripicchio and M. Tiripicchio Camellini, *Angew. Chem., Int. Ed. Engl.*, 1990, **29**, 1140; P. Braunstein, D. Cauzzi, D. G. Kelly, M. Lanfranchi and A. Tiripicchio, *Inorg. Chem.*, 1993, **32**, 3373; W. P. Fehlhammer and M. Fritz, *Chem. Rev.*, 1993, **93**, 1243.

39 D. Fenske, H. Krautscheid, *Angew. Chem., Int. Ed. Engl.*, 1990, **29**, 1452; D. Fenske and J.-C. Steck, *Angew. Chem., Int. Ed. Engl.*, 1993, **32**, 238, and refs. therein.

40 B. A. Frenz, in *Computing in Crystallography*, eds. H. Schenk, R. Olthof-Hazekamp, H. Van Koningveld and G. C. Bassi, Delft University Press, 1978, pp. 64–71.

41 D. T. Cromer and J. T. Waber, *International Tables for X-Ray Crystallography*, Kynoch Press, Birmingham, 1974, vol 4, Tables 2.2b and 2.3.1.

42 C. K. Johnson, ORTEP, Report ORNL 5138, Oak Ridge National Laboratory, Oak Ridge, TN, 1976.

Received 5th *August* 1993; *Paper* 3/04720B